Since January 2020 Elsevier has created a COVID-19 resource centre with free information in English and Mandarin on the novel coronavirus COVID-19. The COVID-19 resource centre is hosted on Elsevier Connect, the company's public news and information website.

Computers in Biology and Medicine 148 (2022) 105847

Contents lists available at ScienceDirect

Computers in Biology and Medicine

journal homepage: www.elsevier.com/locate/compbiomed

An agent-based transmission model of COVID-19 for re-opening policy design

Alma Rodríguez [a,b,c], Erik Cuevas [a,*], Daniel Zaldivar [a], Bernardo Morales-Castañeda [a], Ram Sarkar [d], Essam H. Houssein [e]

[a] Departamento de Electrónica. Universidad de Guadalajara, CUCEI. Av. Revolución 1500, C.P 44430, Guadalajara, Jal, Mexico
[b] Facultad de Ingeniería. Universidad Panamericana, Prolongación Calzada Circunvalación Poniente 49, Zapopan, Jalisco, 45010, Mexico
[c] Desarrollo de Software. Centro de Enseñanza Técnica Industrial, Colomos. Calle Nueva Escocia 1885, Providencia 5a Sección, C.P. 44638, Guadalajara, Jal, Mexico
[d] Department of Computer Science and Engineering, Jadavpur University, Kolkata, 700032, India
[e] Faculty of Computers & Information, Minia University, Minia, 61519, Egypt

ARTICLE INFO

Keywords:
COVID-19
SARS-CoV-2
Transmission model
Agent-based model
Contagion risk

ABSTRACT

The global pandemic caused by the coronavirus (COVID-19) disease has collapsed the worldwide economy. Elements such as non-obligatory vaccination, new strain variants and lack of discipline to follow social distancing measures suggest the possibility that COVID-19 may continue to exist, exhibiting the behavior of a seasonal disease. As the socio-economic crisis has become unsustainable, all countries are planning strategies to gradually restart their economic and social activities. Initially, several containment measures have been adopted involving social distancing, infection detection tests, and ventilation systems. Despite the implementation of such policies, there exists a lack of evaluation of their performance to reduce the contagion index. This means there are no appropriate indicators to decide which intervention or set of interventions present the most effective result. Under these conditions, the development of models that provide useful information in the design and evaluation of containment measures and re-opening policies is of prime concern. In this paper, a novel approach to model the transmission process of COVID-19 in closed environments is proposed. The proposed model can simulate the effects that result from the complex interaction among individuals when they follow a particular containment measure or re-opening policy. With the proposed model, different hypothetical re-opening policies, that are otherwise impossible to analyze in real conditions, can be tested. Computer experiments demonstrate that the proposed model provides suitable information and realistic predictions, which are appropriate for designing strategies that allow a safe return to economic activities.

1. Introduction

Starting in 2020, the World Health Organization [1] declared the outbreak of Severe Acute Respiratory Syndrome Coronavirus 2 (SARS-CoV-2) as a pandemic. The spread of COVID-19 has produced severe social and economic consequences. The strain of SARS-CoV-2 has also experienced recent mutations such as the delta and omicron variants which were first detected with high incidence in India, South Africa, and the United Kingdom. These new changes in the strain have increased its propagation even in countries with high vaccination rates [2,3].

Despite the current vaccination programs against COVID-19, the number of cases along with their social and economic effects continue to be worrisome [4]. Under the present circumstances, vaccination programs present some insufficiencies. Although the period is not clear, the effect of the inoculation is limited [5]. Furthermore, in some countries, vaccination programs are focused only on certain age ranges, and therefore a significant segment of the population is not eligible to get the vaccine. On the other hand, since vaccination is voluntary, a considerable number of people could decline to be immunized [6]. These issues suggest the possibility that COVID-19 may continue to exist, exhibiting the behavior of seasonal disease [7]. Under such conditions, it seems that vaccination programs as a standalone containment measure are not enough to slow down the spread of the disease and its adverse effects. For that reason, international health organizations and governments should be prepared to face this challenge permanently.

The COVID-19 disease has left the whole world facing devastating

* Corresponding author.
E-mail address: erik.cuevas@cucei.udg.mx (E. Cuevas).

https://doi.org/10.1016/j.compbiomed.2022.105847
Received 8 December 2021; Received in revised form 12 May 2022; Accepted 12 May 2022
Available online 19 July 2022

economic damages. The restrictive measures and confinement have forced the lockdown of companies, restaurants, malls, stores, schools, and airlines [8], to mention a few. Additionally, the efforts to control the global pandemic and prevent more infections are breaking global supply chains [9]. As a consequence, unemployment has been mainly impacting vulnerable groups and working-class communities [10]. Therefore, strategies to rebuild the economy are now essential.

The adopted restrictions for containing the spread of COVID-19 have presented a negative effect in the global macroeconomic sector. This fact has forced the design of new re-opening policies that allow interaction among individuals in their workplaces, while at the same time minimizing contagion risk [11]. Such rules represent procedures for activating the economy, which involve prevention measures and security protocols to reduce the contagion risk of COVID-19 [12]. The design of non-pharmaceutical interventions is and will continue as an important tool for reducing the spread of the disease. Currently, a set of impactful measures that limit the propagation of COVID-19 exist. They include air filtration, ventilation, social distancing, contact tracing and random detection testing. The design of these strategies for the new coexistence of people in organizations must be based on information extracted from reliable models rather than just common sense. Mathematical modeling represents an important tool that can be used to compare alternative hypothetical re-opening policies. Valuable time and resources can be saved when re-opening policies are pre-evaluated, by providing a basis to select for consideration only the options which, according to the simulations, deliver the highest benefit.

In the last months, researchers have been confronted with a significant challenge in modeling and forecasting the spread of the COVID-19 disease [13]. They have focused on developing new models that allow the entire community to understand the behavior of the SARS-CoV-2. The primary objective of these models is to provide valuable information to authorities.

Some examples of recent models include the one developed by Ref. [14], where differential equations are formulated to study the dynamics of the virus. The model consists of an autonomous system with realistic assumptions about human populations such as time-dependent classes of susceptibility, exposure, hospitalization, quarantine, recovery, and fatality. The model produces short-term forecasts according to the current governmental policies. However, the model only considers the security measures imposed so far, namely lockdown and social isolation. Moreover, it was only implemented in some states of India.

On the other hand, [15] analyzed the feasibility of restrictive measures, such as isolation and contact tracing, for controlling COVID-19 outbreaks. In the proposed work, the authors developed a stochastic transmission model to quantify the time that the disease can be contained under these security measures. Nevertheless, the model has some limitations since it does not reflect the changes in the transmission process.

In [16], the authors generated a real-time forecast for contagion and risk assessment in specific countries such as the U.K. and France. They implemented a hybrid approach based on an autoregressive integrated moving average model and a Wavelet-based forecasting model. For the risk assessment, they used an optimal regression tree algorithm for fatality rates. The proposed models have some limitations, such as simplification by making assumptions and considering few factors for fatality rates.

Later, [17] proposed a mathematical model for the spread of the COVID-19. The model takes into consideration undetected infectious cases and the sanitary conditions of hospitalized individuals. It also evaluates the necessity of beds in hospitals. However, the model is only appropriate for environments where local community transmission is the leading reason for contagion. Likewise, [18] presented a model for controlling the transmission dynamics of COVID-19. They proposed different control strategies for early and late diagnosis. In addition, the model considers strategies to control the spread of the coronavirus.

Since the origin of the SARS-CoV-2 was in China, several proposed mathematical models emphasize the analysis of the epidemic dynamic in that country, namely the compartmental model proposed by Ref. [19], which studies the spread of the coronavirus considering the transmissibility of super-spreader individuals. Also, [20] developed a model to characterize the dynamics of COVID-19 with un-quarantine infected, confirmed-infected, and quarantine-infected cases. In addition, [21] proposed a mathematical model for evaluating the early transmission dynamics of COVID-19. The model was fitted with datasets of cases in Wuhan and internationally exported cases from Wuhan to predict the coronavirus spread from Wuhan to the rest of the world.

The transmission of a contagious disease in a population is a complex phenomenon. Its behavior is affected mainly by interactions among individuals, rather than simply the characteristics of each isolated individual [22]. Interactions can be observed as social processes [23], such as contact among individuals or their mobility requirements, and as place effects [24], such as the size of the space where the individuals interact or their number. The complexity of the interactions also involves effects through time [25], where results in the past, present, and future influence in the decision-making context; for example, individuals already detected as infected are isolated and no longer represent a contagion source.

Most of the reported schemes use classical modeling approaches to explain, interpret and predict the transmission of COVID-19. These methods consider in their scheme high concentrations of individuals assumed as factors rather than their interactions [26]. Such models are appropriate to interpret the global behavior of COVID-19 on larger scales considering aggregated variables [27]. They cannot provide accurate predictions when it is important to model the transmission process person-to-person [28]. There are several contexts, such as re-opening policy design of closed facilities, where it is critical to analyze the transmission behavior in a finer resolution. These contexts involve small groups of people in facilities where the transmission process is provoked by the interactions among their members [29].

Facilities that operate in closed environments such as schools, factories, or offices present higher rates of infection than those that perform their activities in open or hybrid environments. Cities around the world whose economic sector is mostly represented by closed facilities have higher death rates than average [30], even with good performances of their vaccination programs [31]. Since closed environments involve very different contexts, the type and extension of each intervention should be tailored, depending on the risk of infection, individual behavior presented in each location, economic field, kind of activity, and group of interest [32]. Due to such factors, the study and modeling of the spread of COVID-19 in closed environments require particular attention.

SARS-CoV-2 presents an airborne nature [33]. Therefore, there exists a high risk of infection when people are exposed to inhale microscopic aerosols and respiratory droplets at short distances in closed places. Taking action to reduce the transmission process of COVID-19 is a difficult task since it implies discipline and self-observance of all members of society. Due to the differences among individuals, it is difficult to estimate the real results of the interventions [34]. For that reason, simulating and modeling the COVID-19 transmission risk from a person-to-person perspective is important to predict the epidemiological effects produced from the implementation of intervention actions.

With the aim of reaching their own objectives, organizations integrate the collective work of several individuals. To restrict the number of elements (workers, clients, students, etc.) in an organization reduces its efficiency and the probability of achieving its objectives. An effective re-opening policy, or containment measure, should allow the maximal number of elements inside of a facility under the minimal risk of contagion.

Agent-based models [35] correspond to computational schemes used to explain the behavior of complex systems. Under these models, the actions of elements are emulated inside the system, also considering the manner in which these entities influence and are influenced by their

social and physical environment [36]. Agent-based modeling involves the simulation of individuals making decisions through programmable rules [37]. These rules are defined to include the key aspects of the real scenario to be modeled, along with the particular characteristics of each individual [38]. The rules correspond to the mechanism or process by which the emulated elements make their decisions. They involve the properties of each individual and the physical and social environment [39]. These decisions can affect the properties of the individuals and also influence the common environment. Although the system is modeled from the individual point of view, its main properties are visualized from a global perspective [40]). Agent-based models explicitly involve individual interactions representing their effects on the system results. Even models with elementary elements and simple interactions can produce behaviors that cannot be generated and analyzed from the perspective of classical approaches [41]. Different from traditional mathematical models that assume homogeneous elements, agent-based models consider agents with different properties and deliver more realistic results [42,43].). The powerful modeling properties of the agent-based models have motivated their use in several applications, which include the behavior in supply chains [44], the stock market [45], the characterization of the immune system [46], the understanding about the fall of ancient civilizations [47], and consumer purchasing behavior [48], to name a few.

Agent-based models are particularly appropriate when the behavior of the interacting elements presents an important factor in the results. Hence, its use has also been extended as an option to traditional mathematical approaches to model the behavior of contagious diseases. The results of agent-based models allow to obtain a better fidelity than classical approaches. This fidelity allows extrapolating from model results to real-world system behavior. Therefore, conclusions extracted from the simulations can be used to understand the transmission process and compare policy options. Some agent-based models have been introduced in literature to describe the behavior of different illnesses. Some examples involve schemes such as [49], where historical data is considered to generate interaction patterns for an agent-based model in order to describe the behavior of the influenza epidemic. In Ref. [28], historical information is integrated to predict the plausibility of future disease outbreaks. In Refs. [50,51], two agent-based models are presented, which include interactions to describe the nationwide transmission of influenza in Switzerland and Australia, respectively. Both schemes produce a hypothetical population from census data. Then, agents are operated by some rules that consider interactions among big groups of people. Although all these agent-based approaches incorporate interactions in their models, such interactions are established from a macro resolution (in big groups of people to describe nationwide transmission). For that reason, these models cannot be used in some applications, such as re-opening policy design, where the individual interaction is necessary to evaluate different hypothetical scenarios. More recently, in Ref. [52] a simple agent-based model for transmission risk prediction of COVID-19 in facilities was introduced. The approach models the interaction of agents under simple rules to model the behavior of coronavirus transmission. In spite of its interesting results, it is based on very unrealistic assumptions. The model does not consider recovered cases, the possibility that an agent can be infected outside the facility, or the use of a conventional time index as a base of its computation. As a consequence, the results based on this model cannot provide consistent conclusions to evaluate re-opening policies in facilities.

Recently, other agent-based models have been suggested in literature for evaluating the transmission risk of the COVID-19. In Ref. [53], an agent-based formulation is proposed to emulate the health and economic effects of social distancing interventions. This model analyzes different scenarios of social distancing interventions such as partial isolation or the use of face masks. Since this model uses a SEIR (Susceptible-Exposed-Infected-Recovered) structure with concentrated parameters, it is unable to obtain results of the transmission process from a person-to-person perspective. Other interesting works are proposed in Refs. [54,55]. In both studies, an agent-based approach is presented to evaluate the effect of considering different work schedules to reduce the spread of COVID-19 among construction workers. Finally, in Ref. [56], an approach to model the spread of SARS-CoV-2 in a closed classroom environment is considered. All of these agent-based models present interesting and illustrative examples of transmission risk in different scenarios. However, they are based on very unrealistic assumptions. These models do not consider in their operation important elements such as asymptomatic or vaccinated agents. The influence of asymptomatic or inoculated members in the transmission process is very important. If these factors are not taken into account, the model will produce an overestimation in the number of infected members. Therefore, all these methods have a lack of accuracy in their resulting transmission patterns.

Along with agent-based models, artificial intelligence (AI) and Deep Learning (DL) are two emergent computing areas that have also been used as main elements in different systems for drug discovery, diagnosis and transmission modeling of COVID-19. Most of the conventional methods for drug discovery and vaccine development are not as effective as desired, because they are prone to fail when pathogens are difficult to maintain and characterize under laboratory conditions. In contrast, with the inclusion of AI and DL techniques, the approaches for drug discovery and vaccine development present better results [57], given the opportunity to characterize new active medicaments and antigens through the modeling of their structures extracted from experimental data [58]. These approaches have been extensively considered for drug discovery and vaccine development of COVID-19. Some examples of these systems include the use of deep learning architectures (Ton et al., 2019; [59], multi-task deep models (Hu et al., 2019) and convolutional neural networks (CNN) [60]. The infection diagnosis is also a very important element to reduce COVID-19 transmission. Conventionally, the reverse transcriptase-polymerase chain reaction (RT-PCR) represents the most popular method for COVID-19 detection [61]. Despite its good results, the RT-PCR test presents several associated problems [62,63], such as complexity, dependency on a highly controlled environment and long duration. Recently, approaches of DL have been used to detect COVID-19 from medical images of tomography (CT), magnetic resonance (MRI) or chest x-ray (CXR). These techniques represent a non-invasive test that presents accurate results in a very short time. Some examples of these detectors involve the use of CNN models [64], new DL architectures [65] and DL with metaheuristic techniques [66].

In this paper, we propose a novel agent-based system to model the transmission risk of COVID-19 in facilities. In its model, the system involves three important elements. First, the model characterizes the behavior of the transmission process through the interactions among the individuals within the facility. Second, the model considers the possibility of external infection, which allows associating the contagion dynamic of the locality (city, state, country) with the behavior of the transmission process inside the facility (school, office, factory). Third, the model includes the behavior of asymptomatic and vaccinated agents to increase the accuracy of the resulting transmission patterns. The model analyzes the spread of the disease in specific and limited spaces, namely schools or offices, where the population size can be controlled to evaluate various possible risk scenarios. Different from mathematical models or the already proposed agent-based model for COVID-19 transmission risk, our method provides more realistic results that are helpful for evaluating plausible hypothetical re-opening policies. In order to illustrate its capacities, the proposed model has been applied to the evaluation of several hypothetical re-opening policies, such as: determining the effect of the frequency of the disinfection of surfaces and objects within the facility, obtaining the maximal capacity of individuals in a facility, assessing the effectivity of correct prevention practices imposed in workplaces and measuring the efficiency of restricting the mobility among the individuals inside the facility. The objective of pre-evaluating re-opening policies is to optimize time and resources, by providing a basis to identify which options, according to

the simulations, deliver the highest benefit, so that only the most effective policies are submitted for consideration.

The paper is organized as follows: an introduction to agent-based modeling is presented in section 2. The proposed model is described in section 3. Simulation results are reported in section 4. Finally, conclusions are discussed in section 5.

2. Agent-based modeling

Agent-based models correspond to a new scheme for emulating complex systems with independent components that interact among them. Agents represent artificial elements programmed to accomplish pre-specified procedures [67]. While agents conduct their actions based on their programmed behavior, they interact and compete with other elements in the environment. The type of process executed by an agent is simple. They consider operations from easy choices (such as yes or no actions) to spatial movements. Different from other modeling strategies, agent-based models directly characterize causal relationships in the system, capturing the interactions over time among agents and agents with the environment [68]. This property allows agent-based models to adequately represent systems driven mainly by multiple interactions performed by heterogeneous agents in a common environment. Under such conditions, agent-based models are able to produce sophisticated Spatio-temporal observational relationships among the individuals [69].

The environment in which agents cooperate is a virtual map that can present the structure of a lattice or a multi-dimensional space. In this virtual map, agents can move freely without restriction. Therefore, the environment can be visually analyzed as a physical system [70]. With this property, it can be emulated the evolution of complex systems such as evacuations, traffic, disease transmission, biological systems, etc.

Most agent-based models consider simple rules instead of using complicated behavioral structures or sophisticated architectures. Even though these rules are easy to build and understand, the produced models allow simulating diverse, complex behavioral patterns as a consequence of the cooperation generated among the set of simple agents [71].

The rules characterize the behavior of each individual in an abstract way [67]. It is relatively simple to describe the social and physical interactions among the agents once the relevant elements of the system have been identified. Different types of information can be included in the rules, such as qualitative information, quantitative data, and expert opinions [68]. In rule construction, the idea is to find a trade-off between accuracy and simplicity. The rules need to be simple so that they can capture the main theoretical elements of the system [72]. Although the emphasis on model design is to maintain the rules as simple as possible, it is also determinant to guarantee that the rules meet the required accuracy level. However, too much detail can be counter-productive since it makes it difficult the observation the relationship between the agent and its corresponding behavior [73]. Once the important elements that influence the system have been detected, each must be characterized to represent how the specific properties of the agent and the collective interactions determine the action to be made by the agent.

Definition 1. An agent is an element a_i that involves a set of q internal data $a_i^d = \{p_{i,1}^d, \ldots, p_{i,q}^d\}$. The state and behavior of the agent are determined at a given point of time d by the values of their q internal parameters.

Definition 2. A transition function F is an operator that maps the current state d of an agent a_i to the next one $d+1$ considering a set of conditions $\theta(a_i)$. This process can be formulated as follows:

$$a_i^{d+1} = F\left(a_i^d, \theta\left(a_i^d\right)\right) \tag{1}$$

F represents the combination of a set of m behavioral rules $\{R_1, \ldots, R_m\}$.

Definition 3. A rule R_j ($j \in 1, \ldots, m$) represents an associative scheme that allows the modification of the state for an agent a_i^d if it fulfills certain conditions imposed by $\theta_j(a_i^d)$. In the configuration of a rule R_j, it should be determined two important elements: the condition $\theta_j(a_i^d)$ and the updating mechanism $R_j(a_i^d)$. $\theta_j(a_i^d)$ symbolizes the circumstances in which the rule R_j can be applied to a_i^d while $R_j(a_i^d)$ determines which and to what extent the internal parameters $\{p_{i,1}^d, \ldots, p_{i,q}^d\}$ of a_i^d should be modified. The nature of $R_j(a_i^d)$ could be deterministic or stochastic.

Definition 4. An agent-based model is a computer model that involves a set of N agents $A^d = \{a_1^d, \ldots, a_N^d\}$ where the modification of their internal parameters is performed through a transition function F that includes a set of m rules $\{R_1, \ldots, R_m\}$. It represents the macroscopic state A^d of the system to be modeled in the instant d.

In general, an agent-based model considers the following steps. In the initialization, the agents are configurated in a particular location or state. Then, assuming a specific order (sometimes randomly), every agent a_i ($i \in 1, \ldots, N$) is selected. Afterward, the selected agent a_i is operated through a group of rules that modify its location, state, and association among other agents. These rules model the behaviors of agents when they interact with a realistic environment. Although the system is modeled from the individual point of view, its main properties are visualized from a global perspective. These processes are executed until a certain stop condition has been reached.

The overall procedure of an agent-based model involves two primary operations [74]: the initialization phase and the operation phase. In the initialization phase, a set of agents is configured in an initial state. They might be located in a specific place or arranged with preliminary settings and attributes. After that, the operation phase starts by selecting each agent to update its status. The selection can be random or under a specific order. Every agent is updated according to programmed rules. These rules determine different possible decisions that agents can make. The consequences of the decisions made can change the status of the agent, such as its spatial position, its relationship with other agents, or a modification in any of its attributes. Predefined rules also consider the local influence of neighbor agents in updating the status of each individual. Once all agents have been updated, the operation phase is repeated until a stop criterion is reached. Under this process is how quite complex models can be created using simple rules.

3. The proposed agent-based model

The proposed scheme is an agent-based model to characterize the contagion-recovery process in facilities. It can be used to test control strategies or contention measures. With its use, different hypothetical reopening policies can be tested that are impossible to analyze in real conditions. In this section, the proposed agent-based system to model the COVID-19 contagion risk is described in detail. In concordance with the general procedure of an agent-based model, the description of our method starts with the initialization phase, followed by the operation phase.

3.1. Initialization phase

In this phase, a set A of N agents is defined as:

$$A^d = \left\{a_1^d, \ldots, a_N^d\right\}, \tag{2}$$

where the internal state of every agent is dynamically changing depending on the current day d. Then, these agents are uniformly distributed in a two-dimensional space of size $p \times q$ in order to set their initial spatial position. However, the location of the agents can be arranged differently, depending on the application or context.

Then, the internal parameters of the individuals are established. In the model, we have considered twelve different attributes $a_i^d = \{p_{i,1}^d, \ldots,$

Table 1
Attributes of agents.

P^{I}_{con}	Contagion probability $I = 1, 2, 3$
P_{fat}	Fatality probability
P_{mov}	Movement probability
P_{smo}	Small movements probability
T_{inc}	Incubation time
T_{rec}	Recovery time
S	Infection status
V	Vaccination
As	Asymptomatic condition
RE	Reinfection flag
x	Axis position
y	Axis position

$p^{d}_{i,12}\}$, such as the probability of getting infected (P^{I}_{con}) inside the facility. It adopts three values $(P^{1}_{con}, P^{2}_{con}, P^{3}_{con})$ which depends on the relationship that an individual maintains with the illness: If the agent has not yet been infected P^{1}_{con}, if it has been already infected (reinfection) P^{2}_{con} and if it is already vaccinated P^{3}_{con}. The probability P^{1}_{con} that a susceptible individual gets infected by COVID-19 depends on the local conditions. However, its average value, according to the World Health Organization [1], is within the interval [0.02, 0.03]. Several studies [75] demonstrate that prior infection with COVID-19 protects most people against reinfection. Under these studies, the probability of reinfection P^{2}_{con} of an individual is around 0.0065. COVID-19 vaccines are effective at preventing infection. According to different analyzes [76], the probability of an inoculated individual being infected P^{3}_{con} is around 0.005.

The possibility of external contagion is also considered, which is the risk of infection outside the work environment under analysis. Another included attribute is the probability of a fatal case (P_{fat}), which is based on the Case Fatality Rate (CFR) of the coronavirus disease. The movement probability (P_{mov}), which represents the personal decision of each individual to move freely within the facilities, is also considered in the model. Similarly, we included the likelihood of making a small movement (P_{smo}), which also represents the personal decision to move locally or at a considerable distance. Other important characteristics are the incubation and recovery time. The incubation time (T_{inc}) is the period after contagion and before symptom onset, while the recovery time (T_{rec}) is the required time in quarantine. Furthermore, the infection status (S) of the agents is one of the main characteristics included in the model. Infection status registers the current situation of every individual, namely if the agent is infected, non-infected, in quarantine, or even dead. Finally, we have considered the spatial position of agents in the facility. Another important internal parameter that characterizes an agent is vaccination (V). It is a flag that indicates whether it has been inoculated or not. Another feature is the asymptomatic condition (As) of the agent. It determines whether the agent has the condition of presenting symptoms of the illness or not. The reinfection flag RE is a parameter that indicates if an individual has been previously infected. Under this condition, if the agent is infected again, this implies its reinfection. The final internal parameters of the agent are defined by the x and y coordinates of its position within the facility. A summary of these characteristics is listed in Table 1.

Internal attributes of every agent are assigned with random values within their interval of variation. Nevertheless, for applications, these parameter settings must be configured according to the values reported by the corresponding authorities of each location where the model will be used. Three of the most important internal parameters of an agent are the infection status S, the vaccination V, and the asymptomatic condition As. The infection status S can have three different states 0, 1, -1, and -2, which mean not infected, infected, in quarantine, and dead, respectively. The vaccination parameter V uses the value of one to indicate that the agent has been inoculated. On the contrary, the value of zero means that the individual has not been vaccinated. The asymptomatic condition As adopts the value of one to show that the agent does not present symptoms of COVID-19 once infected. On the other hand, the value of zero implies that the individual presents the typical health manifestations of COVID-19. Finally, the reinfection flag RE allows indicating that an individual has been infected. With the use of this flag, it is possible to differentiate the behavior of individuals that have not been infected from those that have already presented the illness.

Table 2
Simulation parameters.

N	Number of agents or population size
I	The initial number of infected agents
d_{max}	Maximum number of simulation days
M_{max}	Maximum number of movements per day
l_{max}	Maximum length for local movements
R	Distance of contagion
$p \times q$	Facility area
V_N	The number of inoculated elements in N
As_N	The number of asymptomatic agents in N

In addition to the configuration of the internal attributes, simulation parameters must also be initially set. These parameters involve the number of agents N, which represents the population size within the facility; the initial amount of infected agents I, which is an optional parameter that can be considered in the simulations if there are infected agents from the beginning; the maximum number of simulation days d_{max}, which will determine the evolution of the epidemic during a specific time; the maximum number of movements per day M_{max}, which mimics the regular activity of a person on a typical working day; the maximum length for local movements l_{max}, which is the distance of nearby places where it is necessary to go daily, such as the bathroom, the coffee station, the water cooler, etc.; the distances of contagion R, which is the minimum distance for a healthy distance; and the facility area $p \times q$, which is the size of the facility. The other two essential parameters for the simulation are the number of vaccinated individuals V_N and the number of asymptomatic elements As_N present in the population N. The summary of these settings is listed in Table 2.

3.2. Operation phase

In the proposed agent-based model, we have considered six rules $\{R_1, R_2, R_3, R_4, R_5, R_6\}$ to simulate more realistic effects of the coronavirus disease on a closed environment. The first rule R_1 controls the possibility of transmission among sick and healthy agents. The second rule R_2 mimics the mobility and interactions of individuals through the facility. Additionally, the third rule R_3 considers the probability that an agent can be infected outside the facility. Furthermore, the fourth rule R_4 contemplates the incubation time, symptom onset, and quarantine onset. The fifth rule R_5 characterizes the unfortunate fatal cases. Finally, the sixth rule R_5 characterizes the recovery process. These rules represent the main components of modeling the behavior of the COVID-19 disease within a facility. Each rule is explained from the perspective of its execution and processing. From this point of view, it is visualized how rules are applied to all individuals interacting inside the facility. A detailed description of the five rules and the computational procedure for simulation is given in the following subsections.

3.2.1. Rule 1: contagion

According to Refs. [77,78], there is evidence indicating that the COVID-19 viruses are released as microdroplets into the air through coughing, talking and exhalation. These droplets are small enough to float aloft in the air. Therefore, there exists a high risk of the inhalation of droplets (microdroplets) exposed to viruses at short distances between 1 and 2 m of an infected person ([1–4]). Under such conditions, social measures such as physical distancing between individuals must be considered.

Based on the last report on the COVID-19 disease given by the World

Health Organization (Organization, 2020), distancing measures allows for slowing the spread of the disease. Thus, the recommended physical distance is at least 1 m. However, in facilities, colleagues might need to communicate. Consequently, proximity may be indispensable for this communication, exposing themselves to being infected. Hence, rule 1 simulates the contagion risk when individuals interact with each other avoiding a healthy distance.

Under such circumstances, the rule R_1 considers that each agent has a specific probability P^I_{con} of getting infected, which depends on its relationship with the illness. Thus, if a non-infected individual a_i is surrounded by at least one infected neighbor a_j, and the neighbor agent a_j is inside the ratio of contagion distance R, then the individual a_i is prone to be infected by a_j with a probability that depends on the nature of a_i. If the agent a_i has not yet been infected ($RE(a_i) = 0$) and not inoculated ($V(a_i) = 0$), it has a probability of being infected defined by P^1_{con}. In the case of the individual a_i has been already infected ($RE(a_i) = 1$), it maintains a probability P^2_{con} of being infected by a_j. Finally, if a_i is already vaccinated ($V(a_i) = 1$), it presents a contagion probability of P^3_{con}. This rule can be expressed as:

$$S^d(a_i) = \left(rand(0,1) \leq P^I_{con}(a_i)\right)\alpha, \tag{3}$$

where S^d is the current infection status of individual a_i in day d. A random value in the interval of [0,1] is represented by $rand(0,1)$. The term α is the result of the activation function that evaluates the risk of contagion because an infected individual is too close to a_i, which is defined as:

$$\alpha = \begin{cases} 1, & \left(\sum_{j=1,\forall j\neq i}^{N} \left(dist(a_i,a_j) \leq R\right)\beta\right) \geq 1 \\ 0, & otherwise \end{cases} \tag{4}$$

α produces two different values, zero or one, that allow activating or deactivation of the rule. The value of one is produced when an infected agent a_j is closer than a distance R from a_i. Otherwise, the function delivers a value of zero deactivating the rule. In Eq (4), $dist(a_i, a_j)$ is the Euclidian distance between agent a_i and a_j. On the other hand, β is a neighbor activation function that determines if the possible neighbor a_j is infected. Its definition is given as follows:

$$\beta = \begin{cases} 1, & S^d(a_j) > 0 \\ 0, & otherwise \end{cases} \tag{5}$$

β delivers two values. The value one is generated when the agent a_j is infected. If the agent a_j is not infected β will be zero. In the case of the agent a_i had been infected after the operation of rule 1, two different parameters of a_i are modified. The infection status S^d of an agent a_i is changed from 0 to 1.

3.2.2. Rule 2: mobility

Mobility is essential in facilities. It represents one of the main processes of interaction among agents and one of the leading causes of being infected. This rule determines the way in which agents interact spatially in their environment. In the proposed model, each agent has a movement probability P_{mov} that mimics the personal decision to move to another place. Depending on this probability, an agent can move to another location or stay in its current position. Once decided on its movement, the model considers two distinct movement types: displacement to nearby places (local) and movements to distant places (long-distance displacement). Both displacements model the representative movements performed by agents inside the facilities [79,80]. The displacements to nearby places correspond to the most regular movements performed by individuals when they interact in their environment. They represent movements such as taking a tool, making a maneuver, etc. On the other hand, movements to distant places correspond to displacements achieved by the agents when they modify their locations far from their previous position. They correspond to movements such as changes in the work area, visiting a certain department, going to the bathroom, etc. In the model, a local movement is characterized by adding to the current position of an agent a random value within a certain interval $[-l_{max}, l_{max}]$ where l_{max} corresponds to the maximal magnitude of the movement. Contrarily, a long-distance displacement is modeled through a change of position of the agent to a random location inside the facility.

In order to decide the kind of displacement performed by an agent, every agent maintains a probability P_{smo} called small movement probability. Its value allows modeling the particular decision of moving to a nearby place or a distant location. Therefore, under rule two R_2, the position in the x and y axis of agents is changed according to the following expressions:

$$x^{d+1}(a_i) = \begin{cases} X(a_i), & \gamma = 0 \\ x^d(a_i), & otherwise \end{cases} \tag{6}$$

$$y^{d+1}(a_i) = \begin{cases} Y(a_i), & \gamma = 0 \\ y^d(a_i), & otherwise \end{cases} \tag{7}$$

where x^{d+1} and y^{d+1} are the new positions of agent a_i. The current location of the agent a_i is determined by x^d and y^d, while γ is the movement activation function that determines if the agent has decided to move or to remain in the same place, which is defined as:

$$\gamma = \begin{cases} 1, & rand(0,1) \leq P_{mov}(a_i) \\ 0, & otherwise \end{cases} \tag{8}$$

γ produces two values. The value of one is produced if the probabilistic decision is positive. Under such conditions, the agent a_i will experiment with a displacement. The value of zero is delivered when the probabilistic decision is negative, which means that the agent remains in its current position. Terms $X(a_i)$ and $Y(a_i)$ from equations (6) and (7) determine the movement of agents through axis x and y, respectively. If the agent has decided to move, the next decision will be the kind of movement, which can be a small or a distant displacement. Both types of motion for $X(a_i)$ and $Y(a_i)$ can be formulated as in (8) and (9), respectively:

$$X(a_i) = \left(x^d(a_i) + (2(rand(0,1)) - 1)l_{max}\right)\delta + p(rand(0,1))(1-\delta), \tag{9}$$

$$Y(a_i) = \left(y^d(a_i) + (2(rand(0,1)) - 1)l_{max}\right)\delta + q(rand(0,1))(1-\delta), \tag{10}$$

where X and Y correspond to the new position of agent a_i in the x and y axis, respectively. From equation (9), the first term $(x^d(a_i) + (2(rand(0,1)) - 1)l_{max})\delta$ simulates a small movement, where l_{max} is the maximum radius for local movements. In contrast, the second term $p(rand(0,1))(1-\delta)$ mimics moving to a distant place, where p is the size of one side of the.

$p \times q$ facility area. Similarly, the first term from equation (10) corresponds to a small movement, while the second term to the long move, where q is the other side of the $p \times q$ facility area. The small movement activation function δ determines if the agent has decided to make a slight movement or not, which definition is given by:

$$\delta = \begin{cases} 1, & rand(0,1) \leq P_{smo}(a_i) \\ 0, & otherwise \end{cases} \tag{11}$$

Therefore, if $\delta = 1$ represents that the agent a_i will experiment with a small movement; otherwise, the agent a_i experiments a distant displacement. From equation (11), if the value of δ is one, then the second term of equations (9) and (10) becomes zero, which leads to a small movement. On the other hand, if the value of δ is zero, then the first term of equations (9) and (10) becomes zero, causing a distant movement.

3.2.3. Rule 3: external infection

This rule simulates the possibility of an individual being infected outside the facility. Although the proposed agent-based model is introduced to simulate the spread of the COVID-19 in a specific environment, it would not be realistic if the probability of external contagion was not considered. Therefore, this rule simulates what happens beyond the facilities in a general way.

After a regular workday, people are exposed to infection in other places since they may have contact with infected individuals outside the facility. Consequently, the probability of external contagion is considered in the presented model, where agents may start a new workday already infected, putting at risk the health of their colleagues.

Under such considerations, the rule R_3 considers that a non-infected individual a_i can be infected (changing its status to 1) according to a probability that depends on the nature of a_i. If the agent a_i has not yet been infected ($RE(a_i) = 0$) and not inoculated ($V(a_i) = 0$), it has a probability of being infected defined by P^1_{con}. In the case of the individual a_i has been already infected ($RE(a_i) = 1$), it maintains a probability P^2_{con} of being infected by a_j. Finally, if a_i is already vaccinated ($V(a_i) = 1$), it presents a contagion probability of P^3_{con}. Therefore, the external infection rule is modeled as follows:

$$S^{d+1}(a_i) = \begin{cases} 1, \ \left(rand(0,1) \leq P^I_{con}(a_i)\right)\varepsilon > 0 \\ S^d(a_i), \quad otherwise \end{cases}, \tag{12}$$

where ε represents the non-infected test function. It indicates if the agent a_i is or has been infected by the coronavirus disease. ε is formulated as follows:

$$\varepsilon = \begin{cases} 0, \ S^d(a_i) \neq 0 \\ 1, \ otherwise \end{cases} \tag{13}$$

ε produces two different values, zero or one. The value of one is produced if the agent a_i has not been infected so far. Otherwise, the function delivers a value of zero, which means that the agent a_i is or has been infected by COVID-19.

3.2.4. Rule 4: incubation time, symptom onset, and quarantine

According to the last situation report of the COVID-19 disease given by the World Health Organization (Organization, 2020), once an individual has been exposed to the coronavirus, the symptom onset is not immediately. The disease takes a specific time to manifest symptoms. This time is called the incubation time, which ranges on average from 5 to 6 days. On the other hand, asymptomatic individuals that can stand high viral loads remain without presenting any physical symptoms.

In our model, the rule R_4 simulates the process during incubation time, symptom onset, quarantine onset, and the final recovery. An infected individual can be aware after incubation time when symptoms associated with COVID-19 are evident. If symptoms are not severe, the recommendation is household isolation, which corresponds to the quarantine onset. In a favorable scenario, after the quarantine period, recovery is expected.

Information given by the World Health Organization (Organization, 2020) indicates that the incubation time ranges from 5 to 6 days. After that, people experience symptoms within 14 days, which is considered the recovery period in quarantine for mild/moderate symptoms.

Therefore, in the proposed model, an agent firstly is not infected ($S^d(a_i) = 0$). Then, it can be infected as a consequence of its iterations ($S^d(a_i) = 1$). Once infected, if the individual is not asymptomatic ($As(a_i) = 0$), it will be in quarantine ($S^d(a_i) = -1$). If, during the quarantine, the consequences are fatal, the agent dies ($S^d(a_i) = -2$). However, if the individual is asymptomatic ($As(a_i) = 1$), it remains with the condition of infected ($S^d(a_i) = 1$) without presenting a quarantine process.

Based on the presented information, the rule R_4 keeps track of the elapsed days during the incubation time T_{inc} of every not asymptomatic ($As(a_i) = 0$) agent a_i that has been infected. Under such conditions, T_{inc} starts with a value of 6 days. Then, its value is decremented until it assumes the zero value. Thus, the incubation time is updated every day d as follows:

$$T^{d+1}_{inc}(a_i) = \begin{cases} T^d_{inc}(a_i) - 1, \ \left(S^d(a_i) > 0\right) and \ \left(As(a_i) = 0\right) \\ T^d_{inc}(a_i), \quad otherwise \end{cases} \tag{14}$$

When the incubation time is over (after six days), symptoms are evident, so the status of the infected agent change to quarantine ($S^d(a_i) = -1$). Hence, the status update can be expressed as:

$$S^{d+1}(a_i) = \begin{cases} S^d(a_i), \ \left(T^d_{inc}(a_i) > 0\right) and \ \left(As(a_i) = 0\right) \\ -1, \quad otherwise \end{cases} \tag{15}$$

3.2.5. Rule 5: fatal cases

Unfortunately, the COVID-19 disease has left many fatal cases around the world. According to the information collected worldwide from December 2019 to September 2021, the global crude Case Fatality Ratio (CFR), which is the proportion of fatal episodes of illness, is 7% [1]. These cases correspond to infected individuals who experienced severe symptoms due to several underlying medical conditions such as diabetes, hypertension, chronic respiratory disease, cardiovascular disease, and cancer. The risk of severe disease also rises with age. Furthermore, 20% of the cases require hospitalization, while 5% require intensive care and ventilation, impacting health systems. The vaccine for COVID-19 is effective. It can protect people from COVID-19, reducing its fatal effects if they are infected. In general terms, an inoculated person can reduce the acute effects by up 90% [81]. This means that only less than 10% of the vaccinated individual could suffer a fatal case.

Based on the presented information about fatal cases, the proposed model includes a fatality probability P_{fat} for each not inoculated ($V(a_i) = 0$) agent a_i. According to the CFR, this probability ranges from 0 to 0.07. However, if the agent a_i has been vaccinated ($V(a_i) = 0$) such a probability is reduced by a 10% percent ($P_{fat} \cdot 0.1$). Thus, if an individual a_i is in quarantine ($S^d(a_i) = -1$), then this agent can die any day after symptom onset, depending on its CFR and whether it has been inoculated or not. When an agent dies, its status change to $S^d(a_i) = -2$. Hence, R_5 simulates the unfortunate fatal cases under the following expression:

$$S^{d+1}(a_i) = \begin{cases} -2, \ \left(rand(0,1) \leq P_{fat}(a_i)\right) and \ \left(V(a_i) = 0\right) \\ S^d(a_i), \ \left(rand(0,1) \leq P_{fat}(a_i) \cdot 0.1\right) \ and \ \left(V(a_i) = 1\right) \end{cases} \tag{16}$$

where the quarantine activation function σ evaluates if the agent a_i is in the recovery period, expressed as:

$$\sigma = \begin{cases} 1, \ S^d(a_i) = -1 \\ 0, \ otherwise \end{cases} \tag{17}$$

σ produces two values. The value one is generated when the agent a_i is quarantine while it is zero if the agent a_i is in any other state.

3.2.6. Rule 6: recovery process

Once an agent is in quarantine, rule six R_6 considers its recovery process. First, it registers the elapsed days after symptom onset to simulate the recovery period T_{rec}. Then, the infection status S is reset to not infected $S^d(a_i) = 0$. Therefore, T^d_{rec} starts with a value of 14 days. Then, its value is decremented until it assumes the zero value.

$$T^{d+1}_{rec}(a_i) = \begin{cases} T^d_{rec}(a_i) - 1, \ T^d_{rec}(a_i) < 0 \\ T^d_{rec}(a_i), \quad otherwise \end{cases} \tag{18}$$

After 14 days, the quarantine is over. Then, the agent is not infected ($S^d(a_i) = 0.$) anymore. The reinfection flag RE is also set to 1. This means that the agent a_i has been already infected once. Under such conditions, it already has the capacity to be infected again.

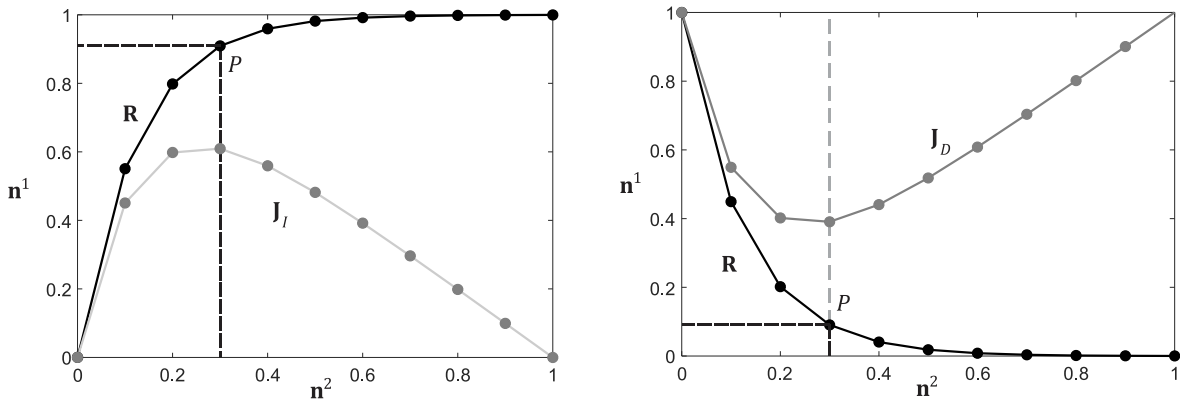

Fig. 1. Two examples for the determination of the significant point: (a) incremental case $\mathbf{J}_I$ (b) decremental case $\mathbf{J}_D$.

3.2.7. Computational procedure

The computational procedure of the model starts with the initialization phase, in which general parameters and the attributes of agents should be configured. Then, the operation phase is executed iteratively until the maximum number of iterations d_{max} has been reached. Every iteration is considered a simulation day that is divided into the time individuals spend inside and outside the facility. Inside the facility, several local movements can be performed by the agents in the facility, which emulate the regular activity of a person on a typical working day. Under such conditions, if an individual changes its position as a consequence of rule two, then it is exposed to contagion by rule one. The maximum number of movements allowed per simulation day is determined by M_{max}. In the process, it is also considered individuals that interact outside the facilities. Thus, the external infection is performed by rule three. Finally, each simulation day finishes when rules four, five, and six are applied. The general procedure is summarized in Algorithm 1. In this paper, the proposed agent model defined in Algorithm 1 has been implemented in MATLAB® code.

Algorithm 1. Computational procedure of the proposed agent-based model.

```
Initialization phase:
|    Set attributes of agents
|    Set simulation parameters
end initialization phase
Operation phase:
|    while the maximum number of simulation days d_max has not been reached
|    |    while the maximum number of movements per day M_max has not been reached
|    |    |    for all agents
|    |    |    |    apply R_1
|    |    |    |    apply R_2
|    |    |    end for
|    |    end while
|    |    for all agents
|    |    |    apply R_3
|    |    |    apply R_4
|    |    |    apply R_5
|    |    |    apply R_6
|    |    end for
|    end while
end operation phase
```

4. Experimental results

In this paper, the proposed model has been developed to compare alternative hypothetical re-opening policies. The option of pre-evaluating re-opening policies allows saving important time and resources, considering only those options which, according to the simulations, deliver the highest benefit.

The experimental section consists of five tests. In the first one (4.1), the generic operation of the model is presented. From the second to fifth test, the proposed model is used to test alternative hypothetical re-opening policies such as (4.2) the effect of the regularity in the disinfection of surfaces and objects, (4.3) the determination of the maximal capacity of individuals in a facility for maintaining a low risk, (4.4) the evaluation of the effectivity in following correct prevention practices, (4.5) the restriction effect of the mobility among the individuals inside the facility and (4.6) discusses the validation of the proposed agent-based model. The objective of all these computer experiments is to illustrate the use of the model to evaluate re-opening policies in simple examples instead of adopting complex contexts. Too much complexity in the scenarios can be counter-productive since it makes it difficult the observation of the produced results. Once the important elements that influence a re-opening policy have been detected, they are emulated in the simplest way. All the computational experiments in this study have been executed in MATLAB® on a PC i5 with a 3 GHz and 12 GB of RAM memory.

To evaluate correctly the results in the computer experiments, the significant point P is adopted as the optimal decision value. It represents the point at which a variable or set of variables reaches a representative behavior. This point is used extensively in the computational test to determine the outbreak end and other essential data in the simulation results. The significant point is the location where the values of a vari-

Table 3
Initial values of the attributes of agents.

Attribute		Value range
Contagion probability	P^1_{con}	[0.02, 0.03]
	P^2_{con}	[0.0060, 0.0065]
	P^3_{con}	[0.0045, 0.0050]
Fatality probability	P_{fat}	[0.007, 0.07]
Movement probability	P_{mov}	[0.3, 0.5]
Small movements probability	P_{smo}	[0.7, 0.9]
Incubation time	T_{inc}	[5, 6]
Recovery time	T_{rec}	14

Table 4
Initial value of simulation parameters.

Parameter		Value
N	Number of agents or population size	200
I	The initial number of infected agents	0
d_{max}	Maximum number of simulation days	365
M_{max}	Maximum number of movements per day	10
l_{max}	Maximum radius for local movements	5 m
R	Distance of contagion	1.5 m
$p \times q$	Facility area	1300 m^2
V_N	The number of inoculated elements in N	50% (100)
As_N	The number of asymptomatic agents in N	40% (80)

able $\mathbf{v}^1$ are no longer critical in terms of its final result in comparison with a second variable $\mathbf{v}^2$ (where the curve visibly bends). The process of computing the significant point P is similar to determining the knee point [38] in engineering. There are not several methods for identifying knee points listed in the literature [57, 58]. Among them, in the proposed approach, we employ the scheme presented in [57] due to its simplicity. Under this scheme, the m values from both variables $\mathbf{v}^1 = \{v^1_1, \ldots, v^1_m\}$ and $\mathbf{v}^2 = \{v^2_1, \ldots, v^2_m\}$ are normalized so that their values range from 0 to 1. This normalization process produces two new variables defined by $\mathbf{n}^1$ and $\mathbf{n}^2$ generated as follows:

$$\mathbf{n}^1 = \frac{\mathbf{v}^1}{v^1_{max}}, \ \mathbf{n}^2 = \frac{\mathbf{v}^2}{v^2_{max}}, \tag{19}$$

where v^1_{max} and v^2_{max} symbolize the maximal values from the variables $\mathbf{v}^1$ and $\mathbf{v}^2$, respectively.

Both normalized variables $\mathbf{n}^1 = \{n^1_1, \ldots, n^1_m\}$ and $\mathbf{n}^2 = \{n^2_1, \ldots, n^2_m\}$ can be related to producing a set of bidimensional points $\mathbf{R} = (\mathbf{r}_1, \ldots, \mathbf{r}_m)$ where each element $\mathbf{r}_w$ ($w \in 1, \ldots, m$) presents the following relationship $\mathbf{r}_w = (n^1_w, n^2_w)$. The relation $\mathbf{R}$ between $\mathbf{n}^1$ and $\mathbf{n}^2$ can be incremental or decremental. $\mathbf{R}$ maintains an incremental behavior if the values of both normalized variables $\mathbf{n}^1$ and $\mathbf{n}^2$ increase as the index of each element $\mathbf{r}_w$ also, increases from 1 to m. On the other hand, $\mathbf{R}$ maintains a decremental behavior when the values of $\mathbf{n}^1$ are reduced as the magnitudes of $\mathbf{n}^2$ increase.

Assuming the normalized information from $\mathbf{n}^1$ and $\mathbf{n}^2$, an objective function $\mathbf{J}$ is defined, which associates the values from $\mathbf{v}^1$ with regard to its significance with $\mathbf{v}^2$. The values of $\mathbf{J}$ depend on the behavior of the relation $\mathbf{R}$. Therefore, $\mathbf{J}$ is computed as follows:

$$\mathbf{J}_I = \mathbf{n}^1 - \mathbf{n}^2, \ \mathbf{J}_D = \mathbf{n}^1 + \mathbf{n}^2, \tag{20}$$

where $\mathbf{J}_I$ represents the computation of $\mathbf{J}$ considering an incremental relation $\mathbf{R}$ while $\mathbf{J}_D$ corresponds to the determination of $\mathbf{J}$ in the case of a decremental case. The objective function $\mathbf{J} = \{J_1, \ldots, J_m\}$ is also a variable of size m. One interesting property of $\mathbf{J}$ is that it has only one global optimum value. This value represents the significant point P, which is calculated as $P = \max(\mathbf{J})$ for the incremental case and $P = \min(\mathbf{J})$ for the decremental scenario.

Fig. 1 illustrates two examples of the determination of the significant point. In the examples, a set of ten points ($m = 10$) that involve the normalized variables $\mathbf{n}^1$ and $\mathbf{n}^2$ is considered. Fig. 1(a) shows the incremental case, while Fig. 1(b) exhibits the decremental scenario.

In this paper, two important indexes are used in the computer experiments outbreak start point *OS* and outbreak endpoint *OE*. The outbreak start point (OS) represents the point (in the number of days) at which the number of infected agents reaches 10% of the total population size N. However, the number of infected agents can be configurated by another percentage or a fixed number of elements F depending on the context to be simulated. On the other hand, the outbreak endpoint (OE) corresponds to the significant point P considering an incremental relation $\mathbf{R}$ between the number of accumulated infected agents ($\mathbf{v}^1$) and the number of days ($\mathbf{v}^2$) obtained by the agent model.

4.1. First test. Simple performance

In the first experiment, the basic performance of the proposed model is exemplified. Under this test, the agent-based model is used to estimate the behavior of the COVID-19 disease. The objective is to obtain valuable information about the evolution of the coronavirus spread within a facility. The computer experiments have been conducted using the parameter settings of Tables 3 and 4, which correspond to the values of the general parameters and the attributes of agents for the initialization phase. From the parameters of Table 3, the elements of the contagion probability (P^I_{con}) are obtained as it is explained in subsection 3.1. On the other hand, the probability of fatal cases (P_{fat}), incubation time (T_{inc}) and recovery time (T_{rec}) have been extracted from (Organization, W. H., 2020). They represent the nominal values from these attributes. On the other hand, the parameters of movement probability (P_{mov}) and small movements probability (P_{smo}) from Table 3 represents the typical values of individual mobility in facilities extracted from Refs. [79,80].

Initially, the status S of all agents is zero since it is considered that there are no infected individuals in the beginning. However, it is possible to configure an initial number of infected individuals I among the population. In this case, it is assumed that they are in incubation time and have not experienced symptoms.

In the initialization phase, the parameter values of the agents are randomly assigned using a uniform distribution considering their specific ranges. Under such conditions, it is generated a heterogeneous population that emulates real conditions. Nevertheless, during the operation phase, the position of the agents is changed according to rule two. Regarding the attributes of the agents, every individual has different probabilities of contagiousness and fatality. Having different probability values within the established ranges simulates the particular characteristics and health conditions of every human being. On the other hand, the incubation time ranges from 5 to 6 days, while the recovery time is set to 14. All these values have been taken from the statistics reported by the WHO. The number of vaccinated individuals within the population is 50%. This value corresponds to the average number of inoculated people around the world, according to the WHO.

Similarly, the probability of movement and small movements are different for every agent. In the simulation, it has been considered that restrictive measures have been adopted. Therefore, these probabilities are limited to a low range. Since agents have mobility restrictions, the possibility that they will move into the facility ranges from 0.3 to 0.5. Besides, the probability that agents move to essential places is higher than displacements to distant places. Thus, the small movement probability ranges from 0.7 to 0.9.

The simulation was conducted for one year (365 days), considering a facility of 300 m^2 and a population of 200 agents. Additionally, it is assumed that an individual makes ten movements on average during a typical 8-h workday. Besides, the maximum radius for a small displacement is considered 5 m. More than 5 m is counted as a distant place. Once the initialization phase is complete, the simulation starts

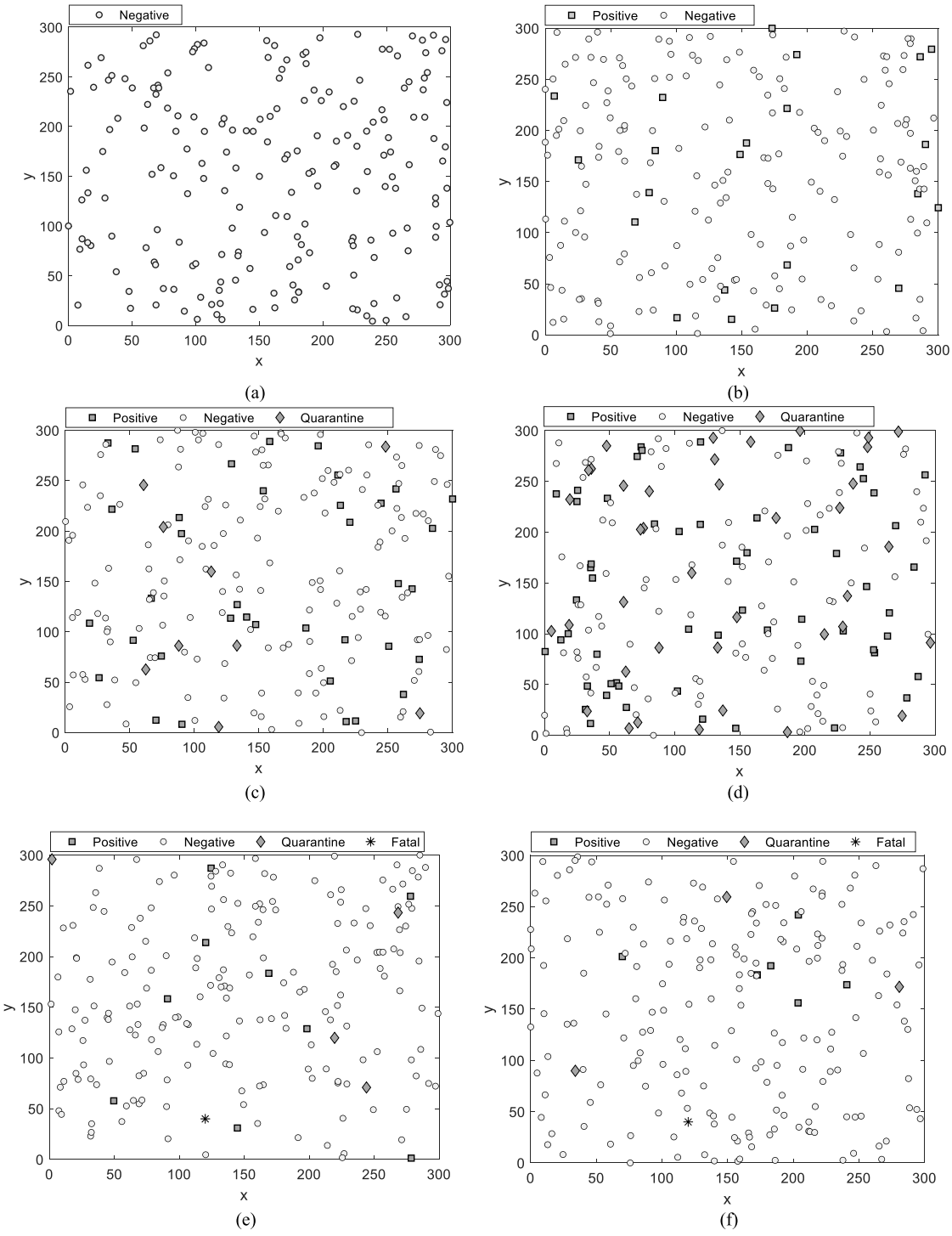

Fig. 2. Simulation evolution of the COVID-19 spread considering different simulation days: (a) day 1, (b) day 5, (c) day 15, (d) day 30, (e) day 90, (f) day 120.

following the procedure reported in Algorithm 1. The Spatio-temporal evolution of the coronavirus spread is shown in Fig. 2, where the status of the agents on different simulation days is illustrated. From Fig. 2, non-infected agents can be identified by circle markers, infected agents by square circles, agents in quarantine by diamond markers, and death agents by asterisk markers. It is important to remark that agents in quarantine (diamond markers) and death agents (asterisk markers) are represented in the spatial-temporal snapshots only for illustration purposes. They do not participate in the emulation process. Their markers are located in their last detected position in the facility. It is assumed that agents in quarantine are insolated (in other different places) while death agents will not be active anymore.

From Fig. 2 (a), it can be observed that all agents are initially non-infected. After five simulation days, Fig. 2(b) shows 22 infected agents, which is a significant number considering that just a few days have elapsed. These results suggest that the coronavirus disease spreads abruptly.

Infected individuals who are in isolation with symptoms can be visualized in Fig. 2 (c). These agents can be identified by diamond markers. It is assumed that the entrance to the work facilities is prohibited for individuals under such conditions. Therefore, agents with a quarantine status can be influenced only by rules four and five, which

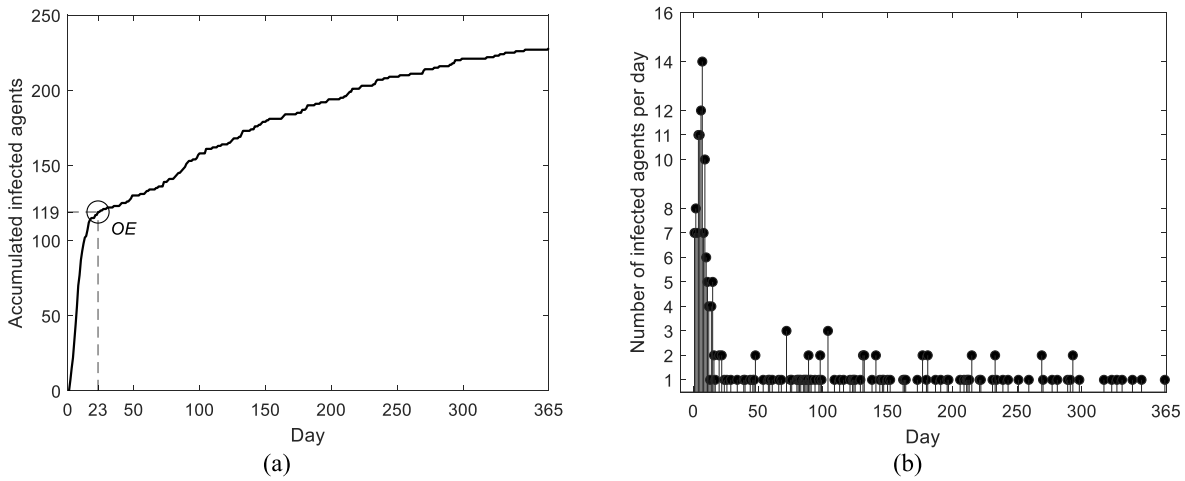

Fig. 3. Analysis of infected cases: (a) accumulated cases and (b) the number of new positive cases per day.

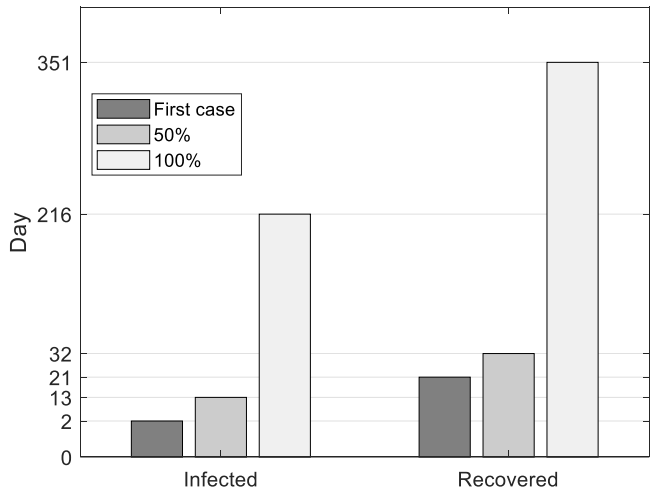

Fig. 4. Comparative of infected, recovered, and fatal cases considering the appearance of the first, 50%, and 100% of the cases.

means that they are under a recovery process outside the facility (either at home or in a hospital) but exposed to being part of the fatal case statistics.

The fatal case takes place approximately from day 90; see Fig. 2. (e). From the figure, one dead agent is illustrated as an asterisk marker. Evidently, the fatal case is excluded from the course of the simulation. It is supposed that recovered agents are back to work but with a reduced probability of getting the coronavirus disease.

Finally, Fig. 2. (f) shows the evolution of the COVID-19 disease after four months of simulation. From the figure, a closer inspection reveals that the number of infected cases has decreased since there are more immune individuals (agents with a very low probability of being infected) and fewer agents in the facility due to those under quarantine, which reduces the probability of new COVID-5 positive cases.

In addition to the evolution of the COVID-19 spread, other useful information is presented. This information includes the accumulated register of infected agents over time, the number of positive cases per day, the accumulated recovered, the number of recovered agents per day, the accumulated fatal cases, the current positive cases, the currently infected individuals in incubation time, and the current agents under quarantine. Since the proposed agent-based model is a stochastic method, the reported results consider the average of 30 independent simulations.

The accumulated COVID-19 positive cases are illustrated in Fig. 3 (a), where it can be observed how the infected agents increase through the days until, eventually, all individuals are infected. The number of infected reaches more than 200 since there are some cases of re-infection. The generated curve clearly shows how the spread of the coronavirus rises rapidly during the first month, which can be considered a critical period in the analysis. The figure illustrates the outbreak

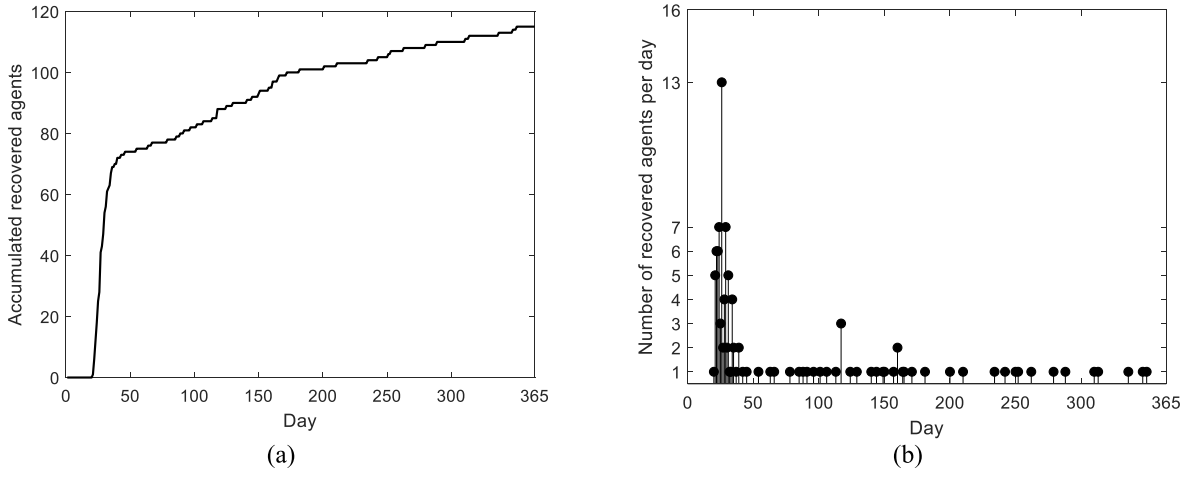

Fig. 5. Analysis of recovered cases: (a) accumulated cases and (b) the number of new recovered instances per day.

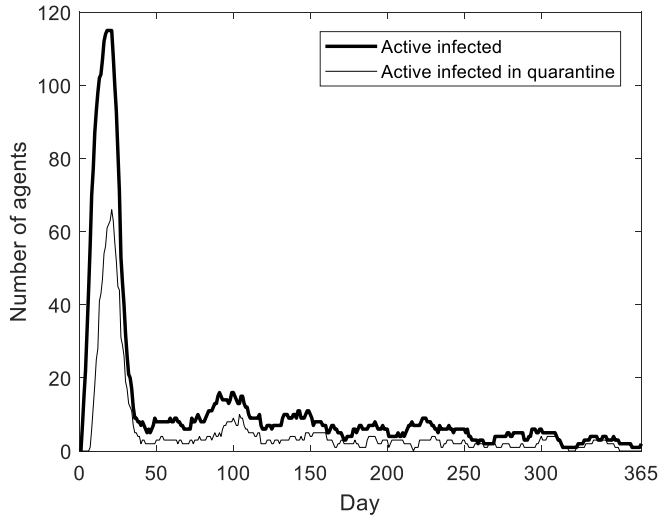

Fig. 6. Evolution of the current infected cases in each simulation day considering the total infected and the agents under quarantine.

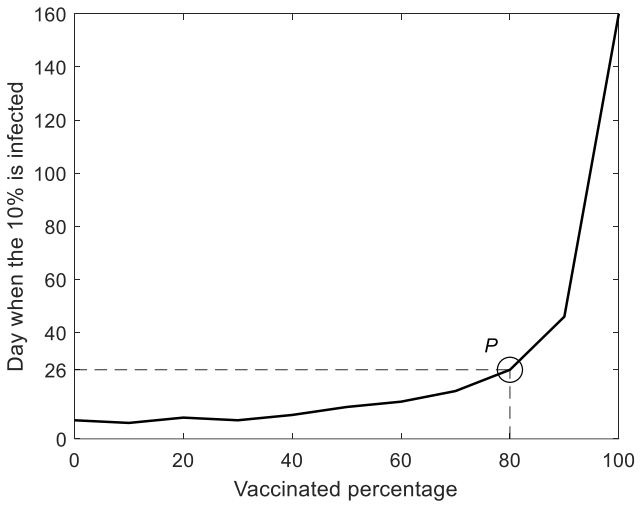

Fig. 7. Results of the second experiment to determine the minimal percentage of vaccinated elements *PorMinVac* to reduce the contagion risk.

endpoint *OE* that characterizes the system response in terms of the number of infected agents. In order to evaluate the size of the outbreak correctly, the number of days in which all the N agents in the facility have been infected cannot be considered a descriptive index since many individuals could maintain a very low probability of being infected (or even immunity). Under such conditions, the number of days required to infect all of the individuals could be longer than necessary to evaluate the duration of the infection in the facility. Therefore, it is defined as the outbreak endpoint *OE*. This point represents the significant point P considering an incremental relation $\mathbf{R}$ between the number of accumulated infected agents ($\mathbf{v}^1$) and the number of days ($\mathbf{v}^2$). Fig. 3(a) exhibits the location of the outbreak endpoint *OE*, which is presented in 23 days. On the other hand, Fig. 3 (b) shows the number of new positive cases per day. From the figure, it can be observed that the maximum number of infected agents per day is 14; this maximum peak is reached approximately at day 20. After one and a half months, the number of infected individuals per day starts to decrease.

Fig. 4 shows the comparative analysis which is reported the day when the first infected individual appears, the time when half of the agents are positive for COVID-19, and the day when all individuals get infected. From this figure, a closer inspection reveals that the first infected case occurs the day 2; half of the agents are positive in approximately 13 days, while all agents were infected by day 216.

The accumulated recovered cases are illustrated in Fig. 5 (a), where it can be observed the evolution of the agents that have successfully overcome the coronavirus disease. Fig. 5 also shows that, at the end of the simulation, not all individuals manage to recover from this illness. Fig. 5 (b) indicates the number of new recovery cases per day. From the figure, it can be observed that the maximum number of recovered agents per day is 13; this maximum peak is reached approximately at day 24. After one and a half months, the number of recovered cases starts to decrease. According to the comparative analysis in Fig. 4, the first recovered cases appear on day 21; 50% of the recovered individuals occur approximately in one month. Besides, 100% of the cases manage to overcome the disease on day 351. On the other hand, there is a fatal case that happens on day 90.

Finally, the behavior of the current infected cases on every simulation day is illustrated in Fig. 6. The figure shows the number of infected agents each day and the evolution of the infected individuals under the quarantine period for each simulation day. From Fig. 6, it can be seen that the number of cases under quarantine is lower than the number of the total infected cases, which is consistent with the number of asymptomatic agents present in the population.

4.2. Second test. Effect of the number of vaccinated elements in a population

The reduction in the risk of contagion of COVID-19 happens if a high number of individuals within a population presents a very low probability of infection. Under such conditions, it is unlikely the transmission from a person-to-person perspective. As a consequence, not only the individuals with a low probability of infection are protected but also the entire population. Therefore, if the number of individuals with a very low probability of being infected is high enough, the spread of the COVID-19 will tend to slow down.

There exist two ways to reduce the probability of COVID-19 infection: Reinfection and inoculation. From the reinfection perspective, the reduction can be attained if a high number of the population has been recovered from COVID-19 developing protective antibodies that avoid future infection. Experts suggest that the transmission risk is reduced when around 80% [82] of the population has recovered from COVID-19. However, the infection of this number of individuals is too high that might provoke several deaths and the collapse of the health system.

The reduction in the transmission of COVID-19 can also be attained through vaccination. Under this mechanism, if enough elements within the population have been inoculated, they develop antibodies that protect them against the infection. Different from the reinfection method, vaccination reduces the transmission risk strongly without provoking the disease or health complications.

In the second test, it is evaluated the influence of inoculated individuals in the population as a mechanism to reduce the probability of infection. The objective of this experiment is to determine the minimum percentage of individuals inside a facility that is necessary to inoculate to reduce the probability of contagion from COVID-19 substantially.

To obtain the minimal percentage of vaccinated elements *PorMinVac* inside of a facility of dimension D, it is considered the following procedure. Firstly, the agent model is configured with the dimension D of the facility. Then, several simulations are conducted, varying the number of vaccinated agents V_N from 0 (0%) to N (100%). For each number of inoculated individuals V_{N_i} within the interval $[0, N]$, a simulation i is executed to evaluate the influence in the transmission risk produced by V_{N_i} individuals interacting inside the facility of dimension D. The transmission risk is evaluated considering the outbreak start point OS, which determines the point where the high rate of contagion starts (in the number of days). Once calculated, the association of each outbreak start point OS_i for each number of inoculated elements V_{N_i}, the minimal percentage of vaccinated elements *PorMinVac* is determined considering

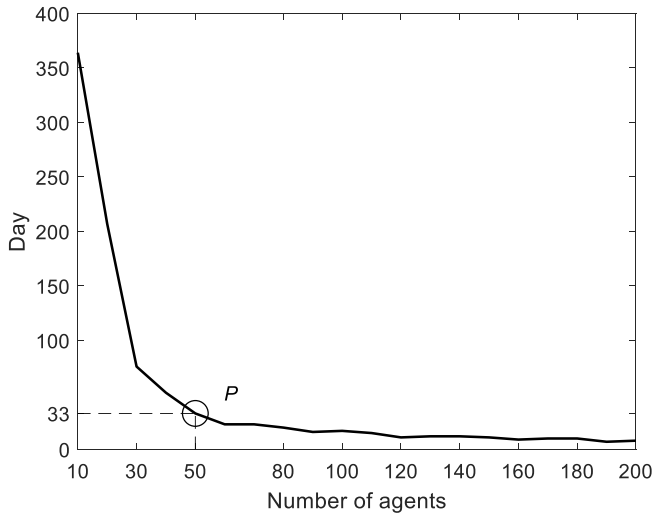

Fig. 8. Results of the third experiment to obtain the capacity of the facility.

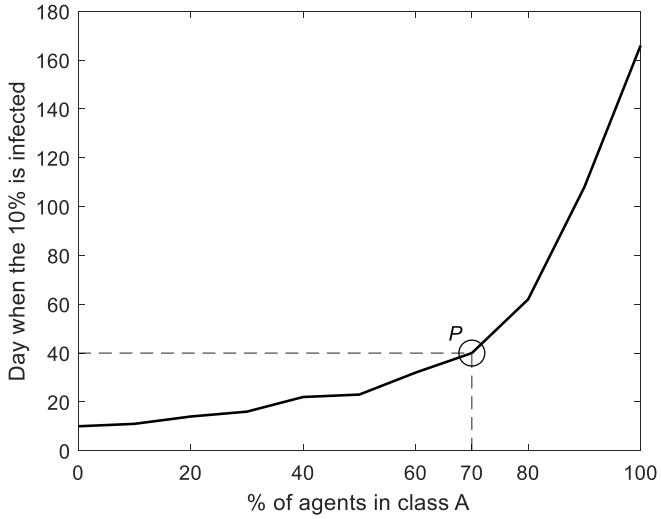

Fig. 9. Results of the fourth experiment to determine the effectiveness of correct prevention practices imposed in workplaces.

the significant point P of the incremental relation $\mathbf{J}_I$ presented by the percentage of vaccinated agents ($\mathbf{v}^1$) and the required number of days ($\mathbf{v}^2$). P represents the location where the number of vaccinated agents V_{N_i} are no longer critical in terms of the transmission risk(where the curve visibly bends).

In each simulation of the experiment, the system is set considering the configuration of Tables 3 and 4 with the parameter V_N varying from 0 (0%) to N (100%). Fig. 7 shows the averaged results of this experiment (30 different independent executions). Therefore, the minimal percentage of vaccinated elements *PorMinVac* inside of a facility that allows reducing the contagion risk is determined considering the significant point P of the incremental relation $\mathbf{J}_I$ presented by the percentage of agents from class I ($\mathbf{v}^1$) and the required number of days ($\mathbf{v}^2$). According to the significant point, it can be seen that more than 80% of vaccinated individuals produce low transmission rates. Under this scenario, when more than 80% of the agents in the workplace are inoculated, the risk of transmission is drastically reduced.

4.3. Third test. Maximal capacity of individuals in a facility

It is evident that the fewer individuals interact in a physical space, the less will be their probability of infection. However, allowing the admission of a very small number of individuals has strong implications regarding the productivity or performance of the workforce by the institution in charge of the facility. In the third test, the proposed model is used to determine the maximal capacity of individuals in a facility maintaining the lowest transmission risk.

To determine the maximal number of individuals max_I inside of a facility of dimension D, it is considered the following procedure. Firstly, the agent model is configured with the dimension D of the facility. Then, several simulations are conducted, varying the number of agents N from a low limit (Low_N) to a high boundary ($Hihgh_N$). Low_N represents a very reduced number of individuals. On the other hand, $Hihgh_N$ symbolizes an exaggerated number of individuals. In order to reduce the number of simulations, it can also be used as $Hihgh_N$ the allowed number of individuals that typically work in the facility (before the COVID outbreak). For each number of individuals N_i within the interval $[Low_N, Hihgh_N]$, a simulation i is executed to evaluate the associated transmission risk produced by N_i individuals interacting inside the facility of dimension D. The transmission risk is assessed considering the outbreak start point OS, which determines the point where the high rate of contagion begins (in the number of days). Once calculated, the association of each outbreak start point OS_i for each N_i, the maximal capacity of individuals max_I is determined considering the significant point P of the decremental relation $\mathbf{J}_D$ presented by the number of agents N_i in the facility ($\mathbf{v}^1$) and the required number of days ($\mathbf{v}^2$) identified by the outbreak start point OS_i. P represents the location where the number of agents N_i are no longer critical in terms of the transmission risk(where the curve visibly bends).

In the third experiment, the number of agents N_i within the facility is varied from 10 (Low_N) to 300 ($Hihgh_N$). In the evaluation, the size D of the facility is set to 300 m^2 only as an example. Then, by using the proposed agent model, the system is simulated in the configuration of Tables 3 and 4, while the outbreak start point OS is registered by each number of individuals N_i. Agent-based models are stochastic approaches. Therefore, in order to eliminate the random effect, each simulation is executed repeatedly 30 times. Under such conditions, the results reflex the averaged outbreak start point OS obtained during the evaluations for each number of agents N_i in the facility.

Fig. 8 shows the association between the number of agents N_i in the facility and the number of days obtained as a result of their respective OS_i values. Therefore, the maximal capacity of individuals max_I in a facility is determined considering the significant point P. From Fig. 8, it is determined that the significant point is obtained when $max_I = 50$. This fact indicates that less than 50 agents in the facility exhibit low transmission rates since the obtained outbreak start points (OS) require a higher number of days to produce the outbreak. Under such circumstances, the facility can maintain less than 50 individuals inside, presenting a very low transmission risk. Contrarily, if the number of individuals N_i is higher than 50, the rates of transmission increase significatively, producing faster outbreaks.

4.4. Fourth experiment. Effectivity of correct prevention practices imposed in workplaces

In the fourth test, the model is used to evaluate the effect of the prevention measurements for diminishing the COVID-19 transmission risk within the workplace. Correct prevention practices to reduce transmission of COVID-19 that can be used in all workplaces involve frequent disinfection with alcohol or hand-washing and the wearing of masks where distancing is not realizable. The consideration of such measures diminishes significatively transmission probability.

In the experiment, each agent a_i from the population A is classified into two types: I) agents that are responsible and follow the prevention practices and II) individuals that are reluctant in this consideration. Since agents from class I follow the prevention measurements strictly, they maintain a low probability of being infected. Under such conditions, each agent from class I, it is assigned a low value of the contagion

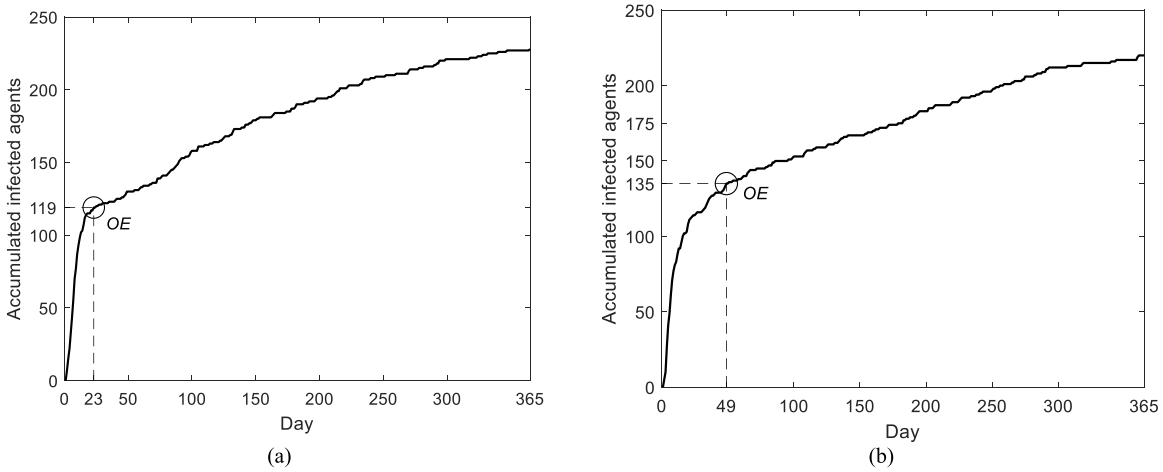

Fig. 10. Outbreak endpoints for the (a) normal and (b) mobility restriction cases.

probability P^I_{con} . Therefore, the P^I_{con} values for all agents from class I are set to 0.0001. On the other hand, P^I_{con} values from the agents of class II, which do not follow the sanitary rules, are generated with random numbers within their typical limits defined in Table 3. Such values represent the standard contagion probabilities inside the workplace.

In the test, it is assessed the importance that a percentage of the agent elements N follows the prevention measurements (class I) in order to reduce the infection probabilities. In the experiment, the percentage of agents from class I varied from 0 to 100% and was deliberately induced inside the population. Then, by using the proposed model, the system is simulated while the outbreak start point *OS* is registered. Excluding the values of P^I_{con} for agents from class I, the remaining parameters are configurated according to Tables 3 and 4

Fig. 9 shows the averaged results of this experiment (30 different independent executions). Therefore, the minimal percentage of agents from class I, which allow reducing the contagion risk, is determined considering the significant point P of the incremental relation $\mathbf{J}_I$ presented by the percentage of agents from class I ($\mathbf{v}^1$) and the required number of days ($\mathbf{v}^2$). According to the significant point, it can be seen that more than 70% of the individuals from class I produce low transmission rates. Under this scenario, when more than 70% of the agents in the workplace are cooperative and follow sanitary measures, the risk of transmission is drastically reduced.

4.5. Fifth experiment. The efficiency of restricting the mobility among the individuals inside the facility

The fifth test, it is evaluated the influence of restricting mobility among the individuals inside the facility through the proposed model. Our agent-based model emulates the basic movements performed by individuals in the facilities. They include local and long-distance displacements. In the model, an agent decides the type of movement in terms of a probabilistic rule. A small displacement is performed with a probability of P_{smo} while a long-distance is achieved with a probability of $(1 - P_{smo})$.

As a re-open policy, it is considered the restriction of mobility. With this restriction, contact among individuals is regulated, reducing the risk of transmission. To evaluate this hypothesis, the probabilities of the proposed model are altered to exclude the long-distance displacements. Therefore, the probability P_{smo} that determines the local movements is set to $P_{smo} = 1$. Under this scenario, the probability of performing long-distance displacements is eliminated $(1 - P_{smo} = 0)$.

In order to contrast the model behavior when the mobility is limited, the analysis considers both cases: a normal case and if the mobility is restricted. In both scenarios, the models are executed considering the parameters of Tables 3 and 4 Nevertheless, in the case of the mobility restriction, the probability P_{smo} is set to 1, discarding the long-distance displacements.

Fig. 10 shows the significant point or outbreak endpoint *OE* for both cases. According to the figure, the outbreak endpoints are about 23 and 49 days for the normal and mobility restriction case, respectively. The more is the amount of days required for the *OE*, the lower will be the contagion risk for the individuals inside the facility. Therefore, it is clear that the re-opening policy of restricting mobility reduces the transmission rate slightly within the workplace. Under this experiment, it is clear that the intervention measurement does not reduce significatively the risk of contagion in comparison to other already contentious practices.

4.6. Validation of the model

Model validation of a computerized model refers to whether the model maintains enough range of accuracy in terms of the domain of its application. Agent-based approaches present several characteristics. They model several internal behaviors of the involved individuals that determine the model operation. There is an absence of comparability between traditional models and those based on agent-based formulations (Bertozzi et al., 2007). There are no empirical data that represent quantitively how should operate several internal processes within an agent-based model. Finally, there is not a standard methodology for building agent-based models. Under such conditions, it is not possible to validate an agent-based model from a traditional perspective.

The most accepted method (Anaya, 2021A; Anaya, 2021B) to validate the performance of agent-based approaches is to relate computationally the results of the agent model with already available actual data. Agent-based approaches model situations that involve different human interactions. Therefore, it is difficult to obtain actual data through real experiments since it is impossible or unethical (infect individuals deliberately). One alternative is to design an experiment with the agent-based model for which there exists information already acquired [83]. This information could be data extracted for other methods, numerical guesses that experts share, etc. Under this direction, in our approach, the agent-based model has been used to reproduce the results of two different cases for which there exists information in the COVID-19 literature. The first case represents determining the minimal percentage of vaccinated elements inside the population to reduce the transmission risk. This value refers to herd immunity, and it is available in the literature. Our approach obtained that it is necessary an 80% of inoculated agents inside the population to reduce the transmission risk, which is the heard immunity reported in several studies [82]. The second case is to evaluate the effectiveness of correct prevention practices imposed in

Table 5
Parameter values for the experiment.

Parameter		Value
N	Number of agents or population size	41,230
I	The initial number of infected agents	0
d_{max}	Maximum number of simulation days	60
M_{max}	Maximum number of movements per day	10
l_{max}	Maximum radius for local movements	5 m
R	Distance of contagion	1.5 m
$p \times q$	Facility area	6.47 Km^2
V_N	The number of inoculated elements in N	80%
As_N	The number of asymptomatic agents in N	40%

workplaces. This value has been evaluated according to several experts. In this case, the proposed agent-based model found that 70% of the individuals must observe the protection intervention to reduce significatively the number of contagions. This result coincides with the value delivered by several studies or suggested by many experts (Anaya, 2021A; Anaya, 2021B).

The most significant problem to validate our method with already available actual data is the lack of appropriate databases. All databases present information on the number of infected people in terms of aggregated variables that accumulate cases in significant regions or countries. Since our approach evaluates the transmission risk from a microscale perspective, it is necessary to use the information of infected members collected from small sections such as universities, facilities, workplaces, and factories. These data are not publicly available. One exception is the information published on (Homepage A) which reports the number of weekly infected members (students, professors, or staff elements) of McGill's University in Canada. The information is updated every Tuesday with confirmed COVID-19 cases reported to McGill's Case Management Group. To evaluate our model, we use these data to compare the result produced by the simulations. From the data presented on (Homepage A), it has been selected the time window from January to February 2022. This period of eight weeks is considered because, during this time, the activities of the university have been declared physically obligatory within the facilities. Under such conditions, the interaction among the members (that is, the main point of the agent-based model) is guaranteed.

To reproduce the actual data from (Homepage A), a computer experiment has been conducted using the parameter settings of Table 5, which correspond to the values of the general parameters and the attributes of the agents during the simulation. Most of these parameter values have been obtained from the official pages of McGill's University.

The number of vaccinated elements V_N has been obtained from (Homepage B). It refers to the percentage of individuals inoculated in Montreal, Canada, where it is located McGill's University. Our model produces, as a result of the simulation, the number of infected people daily. Fig. 11(a) presents the results produced by the agent-based model during the simulation. Since our model is able to predict the number of infected members daily, it is also possible to determine the day of the week in which it is produced the highest number of incidences. Fig. 11 (b) shows a histogram that visualizes the frequency of infected members per day of the week. As can be seen from Fig. 11(b), Wednesday, Tuesday, and Thursday are the days on which the number of infected members is higher than on the weekends.

For the evaluation of our model with the actual data, the information delivered by our model has been integrated to present the incidences weekly. Fig. 12 shows the comparative view between the results predicted by the model and the actual information. An analysis of Fig. 12 demonstrates that the predicted results are quite close to the actual values. Therefore, it is clear that the proposed model can be used to appropriately know the COVID-19 transmission risk from a microscale perspective. To evaluate numerically the accuracy of the predicted values by the proposed model, the mean absolute percentage error (*MAPE*) is calculated. *MAPE* assesses the differences between the predictions of a forecasting method and the real data of the process. *MAPE* is computed as follows:

$$MAPE = \frac{100}{n} \sum_{i=1}^{n} \left| \frac{da_i - P_i}{da_i} \right| \tag{21}$$

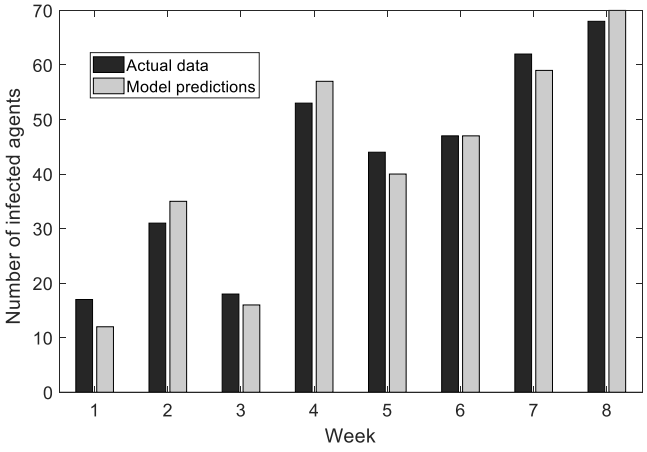

Fig. 12. Comparative view between the results predicted by the model and the actual information.

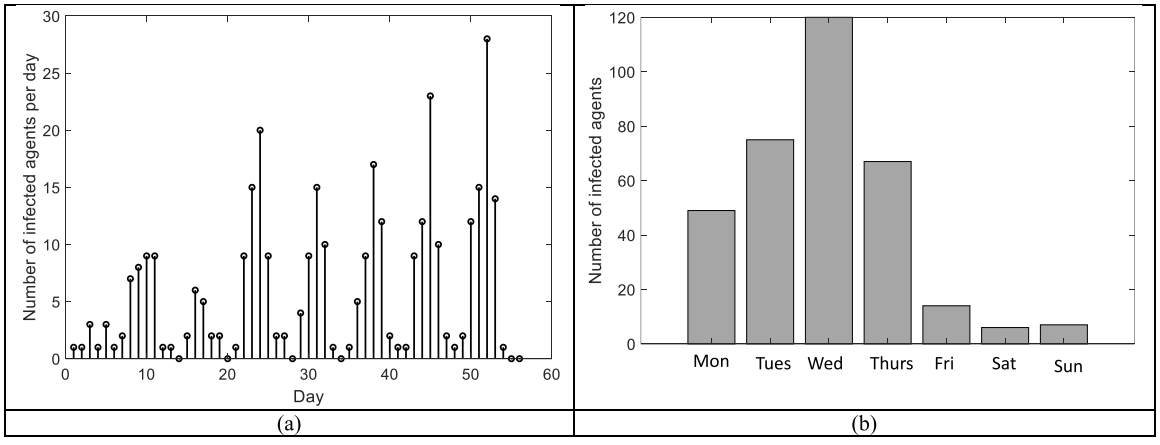

Fig. 11. Simulation results of the agent-based model to predict the information of actual data. 14(a) presents the results produced by the model during the simulation, and 14(b) shows a histogram that visualizes the frequency of infected members per day of the week.

where da_i represents the actual value and P_i symbolizes the predicted value. Their difference is divided by the actual value At. The *MAPE* value obtains its magnitude as the integration of the absolute difference for every predicted point in time and is divided by the number of fitted elements n. Under this index, it can be established that our model maintains a *MAPE* value of 9.7%. Under these results, it is clear that the proposed model allows having excellent predictions about the number of infected members.

5. Conclusions

In this paper, we propose a novel agent-based system to model the transmission risk of the COVID-19 in facilities. In its model, the system involves two important elements. First, the model characterizes the behavior of the transmission process through the interactions among the individuals within the facility. Second, the model considers the possibility of external contagion, which allows associating the contagion dynamic of the locality (city, state, country) with the behavior of the transmission process inside the facility (school, office, factory). The proposed model is capable of simulating the transmission process through the interaction among individuals based on five rules: infection, mobility, external infection, incubation-quarantine-recovery, and fatality. Such rules define the essential behavior of people within the work environment considering their personal decisions and individual health conditions. The proposed model has been developed to compare alternative hypothetical re-opening policies.

In the evaluation, the model has been tested under different contexts. The scenarios involve the effect of the regularity in the disinfection of surfaces and objects, the determination of the maximal capacity of individuals in a facility for maintaining a low risk, the evaluation of the effectivity in following correct prevention practices, and the restriction effect of the mobility among the individuals inside the facility.

From the obtained results, we can conclude that the proposed model provides important information, which is convenient for designing strategies that allow a safe return to economic activities. This model can be included for assistance in the decision-making process since it has the flexibility and scalability to be applied in different scenarios. Furthermore, the setting parameters can be configured according to the specific needs and characteristics of a certain region or environment. With the evaluation of re-opening policies, the proposed model allows saving important time and resources, considering only those options which, according to the simulations, deliver the highest benefit.

There are several research directions that deserve future work. From them, the use of nature-based algorithms to select optimal conditions for a re-opening policy is the most remarkable. Under the current context, there is not enough information to evaluate the effects and the conditions of a re-opening strategy for a determined company or organization on the risk of disease transmission. Therefore, a nature-based approach can be used to find the conditions (solution) that provoke the minimal transmission risk for a simulated re-opening policy. With the use of nature-based methods, it is possible to know the best re-opening strategy from all possible conditions under the simulation of their effects.

Declaration of competing interest

- None of the authors of this paper has a financial or personal relationship with other people or organizations that could inappropriately influence or bias the content of the paper.
- It is to specifically state that "No Competing interests are at stake and there is No Conflict of Interest" with other people or organizations that could inappropriately influence or bias the content of the paper.

References

[1] W.H. Organization, General's opening remarks at the media briefing on COVID-19 - 11 March 2020 [WWW Document], n.d. URL,, https://www.who.int/director-general/speeches/detail/who-director-general-s-opening-remarks-at-the-media-briefing on-covid-19, 2021, 10.10.21.

[2] A. Fontanet, B. Autran, B. Lina, M. Kieny, S. Karim, D. Sridhar, SARS-CoV-2 variants and ending the COVID-19 pandemic, Lancet 397 (2021) 952–954, https://doi.org/10.1016/S0140-6736(21)00370-6.

[3] S. Kashte, A. Gulbake, S. El-Amin III, A. Gupta, COVID-19 vaccines: rapid development, implications, challenges and future prospects, Hum. Cell 34 (2021) 711–733, https://doi.org/10.1007/s13577-021-00512-4.

[4] New Covid-19 Cases Worldwide, Johns Hopkins coronavirus resource center [WWW Document], n.d. URL,, https://coronavirus.jhu.edu/data/new-cases, 2021, 07.11.21.

[5] E. Callaway, COVID super-immunity: one of the pandemic's great puzzles, Nature 598 (7881) (2021) 393–394.

[6] A. Mandavilli, Reaching 'Herd Immunity' Is Unlikely in the U.S., Experts Now Believe, 2021. N. Y. Times.

[7] C. Murray, P. Piot, The potential future of the COVID-19 pandemic: will SARS-CoV-2 become a recurrent seasonal infection? J. Am. Med. Assoc. 325 (2021) 1249–1250, https://doi.org/10.1001/jama.2021.2828, 2021.

[8] S.M. Iacus, et al., Estimating and projecting air passenger traffic during the COVID-19 coronavirus outbreak and its socio-economic impact, Saf. Sci. 129 (2020), 104791, https://doi.org/10.1016/j.ssci.2020.104791.

[9] D. Ivanov, Predicting the impacts of epidemic outbreaks on global supply chains: a simulation-based analysis on the coronavirus outbreak (COVID-19/SARS-CoV-2) case, Transport. Res. E Logist. Transport. Rev. 136 (2020), 101922, https://doi.org/10.1016/j.tre.2020.101922.

[10] D.L. Blustein, et al., Unemployment in the time of COVID-19: a research agenda, J. Vocat. Behav. 119 (2020), 103436, https://doi.org/10.1016/j.jvb.2020.103436.

[11] W. Mckibbin, R. Fernando, Crawford school of public policy CAMA centre for applied macroeconomic analysis the brookings institution centre of excellence in population ageing research the global macroeconomic impacts of COVID-19, Seven Scenarios Seven Scenar.*' 2 (4) (2020) 12–22. Available at: https://ssrn.com/abstract=3547729.

[12] G. Li, R. Hu, X. Gu, 'A close-up on COVID-19 and cardiovascular diseases', Nutrition, metabolism, and cardiovascular diseases : NMCD. 2020/04/08. The Italian Diabetes Society, the Italian Society for the Study of Atherosclerosis, the Italian Society of Human Nutrition and the Department of Clinical Medicine and Surgery, Federico II University 30, Published by Elsevier B.V, 2020, pp. 1057–1060, https://doi.org/10.1016/j.numecd.2020.04.001, 7.

[13] A.L. Bertozzi, et al., The Challenges of Modeling and Forecasting the Spread of COVID-19, 2020.

[14] M. Mandal, et al., 'A Model Based Study on the Dynamics of COVID-19: Prediction and Control', *Chaos*, 136, Solitons & Fractals, 2020, 109889, https://doi.org/10.1016/j.chaos.2020.109889.

[15] J. Hellewell, et al., Feasibility of controlling COVID-19 outbreaks by isolation of cases and contacts, Lancet Global Health 8 (4) (2020) e488–e496, https://doi.org/10.1016/S2214-109X(20)30074-7.

[16] T. Chakraborty, I. Ghosh, Real-time forecasts and risk assessment of novel coronavirus (COVID-19) cases: a data-driven analysis, Chaos, Solit. Fractals 135 (2020), 109850, https://doi.org/10.1016/j.chaos.2020.109850.

[17] B. Ivorra, et al., Mathematical modeling of the spread of the coronavirus disease 2019 (COVID-19) taking into account the undetected infections. The case of China, Commun. Nonlinear Sci. Numer. Simulat. 88 (2020), 105303, https://doi.org/10.1016/j.cnsns.2020.105303.

[18] S.E. Moore, E. Okyere, Controlling the Transmission Dynamics of COVID-19, 2020.

[19] F. Ndaïrou, et al., 'Mathematical Modeling of COVID-19 Transmission Dynamics with a Case Study of Wuhan', *Chaos*, 135, Solitons & Fractals, 2020, 109846, https://doi.org/10.1016/j.chaos.2020.109846.

[20] S. Zhao, H. Chen, Modeling the epidemic dynamics and control of COVID-19 outbreak in China, Quantitative Biology 8 (1) (2020) 11–19, https://doi.org/10.1007/s40484-020-0199-0.

[21] A.J. Kucharski, et al., Early dynamics of transmission and control of COVID-19: a mathematical modelling study, Lancet Infect. Dis. 20 (5) (2020) 553–558, https://doi.org/10.1016/S1473-3099(20)30144-4.

[22] D.A. Luke, K.A. Stamatakis, Systems science methods in public health: dynamics, networks, and agents, Annu. Rev. Publ. Health 33 (1) (2012) 357–376.

[23] L.F. Berkman, T. Glass, I. Brissette, T.E. Seeman, From social integration to health: durkheim in the new millennium, Soc. Sci. Med. 51 (6) (2000) 843–857.

[24] S. Macintyre, A. Ellaway, S. Cummins, Place effects on health: how can we conceptualise, operationalise and measure them? Soc. Sci. Med. 55 (1) (2002) 125–139.

[25] H. Rutter, N. Savona, K. Glonti, J. Bibby, S. Cummins, D.T. Finegood, F. Greaves, L. Harper, P. Hawe, L. Moore, M. Petticrew, E. Rehfuess, A. Shiell, J. Thomas, M. White, The need for a complex systems model of evidence for public health, Lancet 390 (10112) (2017) 2602–2604.

[26] E.R. Smith, F.R. Conrey, Agent-based modeling: a new approach for theory building in social psychology, Pers. Soc. Psychol. Rev. 11 (1) (2007) 87–104.

[27] W.C. Roda, et al., Why is it difficult to accurately predict the COVID-19 epidemic? Infectious Dis. Model. 5 (2020) 271–281, https://doi.org/10.1016/j.idm.2020.03.001.

[28] T.C. Germann, et al., Mitigation strategies for pandemic influenza in the United States, Proc. Natl. Acad. Sci. USA 103 (15) (2006) 5935, https://doi.org/10.1073/pnas.0601266103. LP – 5940.

[29] H. Qi, S. Zhang, X. Meng, H. Dong, Periodic solution and ergodic stationary distribution of two stochastic SIQS epidemic systems, Physica A 508 (2018) 223–241.

[30] D. Ivory, R. Gebeloff, S. Mervosh, Young People Have Less Covid-19 Risk, but in College Towns, Deaths Rose Fast, The New York Times, 2020.
[31] L. Gostin, D. Salmon, H. Larson, Mandating COVID-19 vaccines, J. Am. Med. Assoc. 325 (2021) 532–533, https://doi.org/10.1001/jama.2020.26553.
[32] D. Valencia, Brief review on COVID-19: the 2020 pandemic caused by SARS-CoV-2, Cureus 12 (2021), https://doi.org/10.7759/cureus.7386.
[33] M. Klompas, M. Baker, C. Rhee, Airborne transmission of SARS-CoV-2: theoretical considerations and available evidence, J. Am. Med. Assoc. 324 (2020) 441–442, https://doi.org/10.1001/jama.2020.12458.
[34] M. Ribeiro, R. da Silva, V. Mariani, L. dos Santos Coelho, Short-term Forecasting Covid-19 Cumulative Confirmed Cases: Perspectives for brazil, Chaos, Solitons & Fractals, 2020, p. 109853.
[35] C.M. Macal, M.J. North, Tutorial on agent-based modelling and simulation, J. Simulat. 4 (3) (2010) 151–162, https://doi.org/10.1057/jos.2010.3. Taylor & Francis.
[36] E. Bonabeau, Agent-based modeling: methods and techniques for simulating human systems, Proc. Natl. Acad. Sci. USA 99 (suppl 3) (2002) 7280–7287.
[37] J.M. Epstein, Generative Social Science: Studies in Agent-Based Computational Modeling, Princeton University Press, Princeton, NJ, 2006.
[38] N. Gilbert, Agent-Based Models, Sage Publications, Los Angeles, 2008.
[39] S.F. Railsback, V. Grimm, Agent-Based and Individual-Based Modeling: A Practical Introduction, Princeton University Press, New Jersey, 2011.
[40] J. Badham, E. Chattoe-Brown, N. Gilbert, Z. Chalabi, F. Kee, R. Hunter, Developing agent-based models of complex health behaviour, Health Place 54 (2018) 170–177.
[41] N. Gilbert, K. Troitzsch, Simulation for the Social Scientist, second ed., Open University Press, Maidenhead, UK, 2005.
[42] J. Badham, Functionality, accuracy, and feasibility: talking with modelers, J. Policy Complex Syst. 1 (2) (2014) 60–87.
[43] H. Sayama, Introduction to the modeling and analysis of complex systems. Open SUNY textbooks, URL, https://textbooks.opensuny.org/introduction-to-themodeling-and-analysis-of-complex-systems/, 2015.
[44] C. Macal, D. Sallach, M. North, Emergent structures from trust relationships in supply chains, in: Proc. Agent 2004: Conf. On Social Dynamics, 2004, pp. 7–9.
[45] W. Arthur, S. Durlauf, D. Lane, The Economy as an Evolving Complex System II, 1997, p. 11.
[46] V.A. Folcik, G.C. An, C.G. Orosz, The Basic Immune Simulator: an agent-based model to study the interactions between innate and adaptive immunity, Theor. Biol. Med. Model. 4 (1) (2007) 39, https://doi.org/10.1186/1742-4682-4-39.
[47] T.A. Kohler, G.J. Gumerman, R.G. Reynolds, Simulating ancient societies, Sci. Am. JSTOR 293 (1) (2005) 76–84.
[48] M.J. North, et al., Multiscale agent-based consumer market modeling, Complexity 15 (5) (2010) 37–47, https://doi.org/10.1002/cplx.20304.
[49] T. Smieszek, et al., Reconstructing the 2003/2004 H3N2 influenza epidemic in Switzerland with a spatially explicit, individual-based model, BMC Infect. Dis. 11 (1) (2011) 115, https://doi.org/10.1186/1471-2334-11-115.
[50] M. Marini, et al., Enhancing response preparedness to influenza epidemics: agent-based study of 2050 influenza season in Switzerland, Simulat. Model. Pract. Theor. 103 (2020), 102091, https://doi.org/10.1016/j.simpat.2020.102091.
[51] O.M. Cliff, et al., Investigating spatiotemporal dynamics and synchrony of influenza epidemics in Australia: an agent-based modelling approach, Simulat. Model. Pract. Theor. 87 (2018) 412–431, https://doi.org/10.1016/j.simpat.2018.07.005.
[52] E. Cuevas, An agent-based model to evaluate the COVID-19 transmission risks in facilities, Comput. Biol. Med. 121 (May) (2020), 103827, https://doi.org/10.1016/j.compbiomed.2020.103827. Elsevier Ltd.
[53] P. Silva, P. Batista, H. Lima, M. Alves, F. Guimarães, R. Silva, COVID-ABS: an agent-based model of COVID-19 epidemic to simulate health and economic effects of social distancing interventions, Chaos, Solitons & Fractals 139 (2020), 110088.
[54] F. Anaya, Modeling working shifts in construction projects using an agent-based approach to minimize the spread of COVID-19, J. Build. Eng. 41 (2021), 102413.
[55] F. Anaya, Modeling the spread of COVID-19 on construction workers: an agent-based approach, Saf. Sci. 133 (2021), 105022.
[56] R. Zafarnejad, P. Griffin, Assessing school-based policy actions for COVID-19: an agent-based analysis of incremental infection risk, Comput. Biol. Med. 134 (2021), 104518.
[57] M.B. Jamshidi, et al., Deep learning techniques and COVID-19 drug discovery: fundamentals, state-of-the-art and future directions, in: I. Arpaci, M. Al-Emran, A. M. Al-Sharafi, G. Marques (Eds.), Emerging Technologies during the Era of COVID-19 Pandemic. Studies in Systems, Decision and Control, 348, Springer, Cham, 2021.
[58] B. Chen, et al., Predicting HLA class II antigen presentation through integrated deep learning, Nat. Biotechnol. 37 (11) (2019) 1332–1343.
[59] M.B. Jamshidi, et al., Artificial Intelligence and COVID-19: deep learning approaches for diagnosis and treatment, IEEE Acc 8 (2020) 109581–109595.
[60] A. Muneer, S. Mohamed, N. Arifin, D. Agustriawan, S. Wahyudie, iVaccine-Deep: Prediction of COVID-19 mRNA Vaccine Degradation Using Deep Learning, Journal of King Saud University, Computer and Information Sciences, 2022. In Press.
[61] N. Jawerth, How is the COVID-19 virus detected using real time RT–PCR? IAEA Bull. 61 (2) (2020) 8–11.
[62] J. Won, S. Lee, M. Park, T. Kim, M. Park, B. Choi, D. Kim, H. Chang, W. Heo, V. Kim, C. Lee, Development of a laboratory-safe and low-cost detection protocol for SARS-CoV-2 of the Coronavirus Disease 2019 (COVID-19), Exper. Neurobiol. 29 (2) (2020) 107–119.
[63] L. Wang, Z. Lin, A. Wong, COVID-Net: a tailored deep convolutional neural network design for detection of COVID-19 cases from chest X-ray images, Sci. Rep. 10 (1) (2020), 19549.
[64] H. Hosseinzadeh, Deep Multi-View Feature Learning for Detecting COVID-19 Based on Chest X-Ray Images, Biomedical Signal Processing and Control, 2022. In Press.
[65] J.L. Gayathri, A. Bejoy, M. Sujarani, S. Nairb, A computer-aided diagnosis system for the classification of COVID-19 and non-COVID-19 pneumonia on chest X-ray images by integrating CNN with sparse autoencoder and feed forward neural network, Comput. Biol. Med. 141 (2022), 105134.
[66] S. Chakraborty, A. Saha, S. Nama, S. Debnath, COVID-19 X-ray image segmentation by modified whale optimization algorithm with population reduction, Comput. Biol. Med. 139 (2021), 104984.
[67] W.K.V. Chan, Y. Son, C.M. Macal, Agent-based simulation tutorial - simulation of emergent behavior and differences between agent-based simulation and discrete-event simulation, in: Proceedings of the 2010 Winter Simulation Conference, 2010, pp. 135–150, https://doi.org/10.1109/WSC.2010.5679168.
[68] Z. Chalabi, T. Lorenc, Using agent-based models to inform evaluation of complex interventions: examples from the built environment, Prev. Med. 57 (5) (2013) 434–435.
[69] L. An, Modeling human decisions in coupled human and natural systems: review of agent-based models, Ecol. Model. 229 (2012) 25–36.
[70] S.D. Angus, B. Hassani-Mahmooei, Anarchy" Reigns: a quantitative analysis of agent-based modelling publication practices in JASSS, 2001–2012, J. Artif. Soc. Soc. Simulat. 18 (4) (2015) 16.
[71] F. Bianchi, F. Squazzoni, Agent-based models in sociology, WIREs Comput. Stat. 7 (4) (2015) 284–306.
[72] D. O'Sullivan, T. Evans, S. Manson, S. Metcalf, A. Ligmann-Zielinska, C. Bone, Strategic directions for agent-based modeling: avoiding the YAAWN syndrome, J. Land Use Sci. 11 (2) (2015) 177–187.
[73] M.A. Janssen, The practice of archiving model code of agent-based models, J. Artif. Soc. Soc. Simulat. 20 (1) (2017) 2.
[74] E. Silverman, Methodological Investigations in Agent-Based Modelling, Springer International Publishing, Cham, Switzerland, 2018.
[75] A. Okhuese, Estimation of the probability of reinfection with COVID-19 by the susceptible-exposed-infectious-removed-undetectable-susceptible model, JMIR Public Health Surveill 6 (2) (2020), e19097, 2020 05 13.
[76] P. Knobel, C. Serra, S. Grau, R. Ibañez, P. Diaz, O. Ferrández, R. Villar, A. Lopez, N. Pujolar, J. Horcajada, M. Roman, M. Comas, M. Sala, X. Castells, Coronavirus disease 2019 (COVID-19) mRNA vaccine effectiveness in asymptomatic healthcare workers, Infect. Control Hosp. Epidemiol. 2021 (2021) 1–2.
[77] S. Hamid, M.Y. Mir, G.K. Rohela, Novel coronavirus disease (COVID-19): a pandemic (epidemiology, pathogenesis and potential therapeutics), New Microbes and New Infections 35 (2020), 100679, https://doi.org/10.1016/j.nmni.2020.100679.
[78] S. Chavez, et al., Coronavirus Disease (COVID-19): a primer for emergency physicians, Am. J. Emerg. Med. (2020), https://doi.org/10.1016/j.ajem.2020.03.036.
[79] M. Wardhana, Spatial analysis of users movement pattern and its socialization on public facilities and environment through the ESVA, Procedia Social Behavioral Sci. 227 (2016) 101–106.
[80] J. Steen, H. Markhede, Spatial and social configurations in offices, J. Space Sintax 1 (1) (2010) 121–132.
[81] E. Azak, A. Karadenizli, K. Uzuner, N. Karakaya, N. Zafer, S. Hulagu, Comparison of an inactivated Covid19 vaccine-induced antibody response with concurrent natural Covid19 infection, Int. J. Infect. Dis. 113 (2021) 58–64.
[82] C. Aschwanden, Five reasons why COVID herd immunity is probably impossible, Nature 591 (2021) 520–522.
[83] G. Fagiolo, C. Birchenhall, P. Windrum, Empirical validation in agent-based models: introduction to the special issue, Comput. Econ. 30 (3) (2007) 189–194.